NASA Technical Memorandum 110343

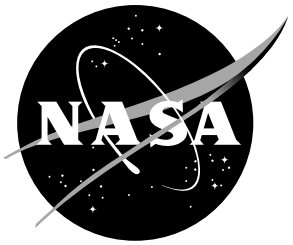

A Candidate Wake Vortex Strength Definition for Application to the NASA Aircraft Vortex Spacing System (AVOSS)

David A. Hinton
Langley Research Center, Hampton, Virginia

Chris R. Tatnall
George Washington University
Joint Institute for Advancement of Flight Sciences
Langley Research Center, Hampton, Virginia

September 1997

National Aeronautics and
Space Administration
Langley Research Center
Hampton, Virginia 23681-0001

Summary

A significant effort is underway at NASA Langley to develop a system to provide dynamical aircraft wake vortex spacing criteria to Air Traffic Control (ATC). The system under development, the Aircraft Vortex Spacing System (AVOSS), combines the inputs of multiple subsystems to provide separation matrices with sufficient stability for use by ATC and sufficient monitoring to ensure safety. The subsystems include a meteorological subsystem, a wake behavior prediction subsystem, a wake sensor subsystem, and system integration and ATC interfaces. The proposed AVOSS is capable of using two factors, singly or in combination, for reducing in-trail spacing. These factors are wake vortex motion out of a predefined approach corridor and wake decay below a significant strength. Although basic research into the wake phenomena has historically used wake total circulation as a strength parameter, there is a requirement for a more specific strength definition that may be applied across multiple disciplines and teams to produce a real-time, automated system. This paper presents some of the limitations of previous applications of circulation to aircraft wake observations and describes the results of a preliminary effort to bound a spacing system strength definition.

Acknowledgments

The work presented here draws on the contributions of a number of individuals. Dr. Roland Bowles provided the basis for interpreting wake strength measurements in terms of a two vortex system, rather than attributing the measurement to the vortex under observation, as well as the concept of considering the wake torque on a flat plate as a possible strength measure. Dr. Rich Heinricks of MIT Lincoln Laboratory performed analysis to quantify the differences between sensed wake strengths measured by the Lincoln CW Lidar and the theoretical values for the aircraft observed at Memphis, as explained by the two vortex system consideration. Mr. Craig Watry, an Air Force Academy graduate temporarily assigned to Langley in 1994, performed much analysis with the data collected at Idaho Falls in 1990 to show the sensitivity of perceived wake characteristics to different model fit assumptions. Dr. Fred Proctor, whose Terminal Area Simulation System (TASS) numeric model is the primary tool within the Terminal Area Productivity Program for understanding wake behavior in the atmosphere, contributed to the understanding of the variations between different definitions of circulation and how those variations affect interpretation of field data and numeric model results.

Introduction

A significant effort is underway at NASA Langley, as an element of the NASA Terminal Area Productivity (TAP) Program, to develop a system to provide dynamical aircraft wake vortex spacing criteria to Air Traffic Control (ATC). The system under development, the Aircraft Vortex Spacing System (AVOSS) is described in references 1 and 2. The AVOSS system combines the inputs of multiple subsystems to provide separation matrices with sufficient stability for use by ATC and sufficient monitoring to ensure safety. The subsystems include a meteorological subsystem, a wake prediction subsystem, a wake sensor subsystem, and system integration and ATC interfaces.

The proposed AVOSS is capable of using two factors, singly or in combination, for reducing in-trail spacing. These factors are wake vortex motion out of a predefined approach corridor and wake decay below a strength that is operationally significant. The first factor requires no knowledge of aircraft interactions with wakes, as the wake has been removed from the approach corridor. The second factor requires knowledge of wake decay rates, aircraft/wake interactions, and sensor observable characteristics of wakes. There is a system requirement to define a wake strength parameter whose decay rate can be predicted, that scales to the operational significance of an aircraft encounter, and that can guide the development of practical sensors. This requirement arises from the consideration that coordination of multiple disciplines and teams is required for successful development, including the fields of meteorology, computational fluid dynamics (CFD), computer science, aeronautical, electro-optical and RF remote sensor technology, system integration, human factors, ATC procedures, and airport operations. A common definition of vortex strength is needed to coordinate the results of CFD modeling for wake decay, aircraft/wake interaction studies, field data interpretation, and wake sensor design. This paper describes the results of a preliminary effort to determine a strength definition.

Abbreviations

ATC	Air Traffic Control
AVOSS	Aircraft Vortex Spacing System
CFD	Computational Fluid Dynamics
CW	Continuous Wave
DOF	Degrees of Freedom
FAA	Federal Aviation Administration
MIT	Massachusetts Institute of Technology
TAP	Terminal Area Productivity
TASS	Terminal Area Simulation System

Symbols

AR	Aspect Ratio.
b	Aircraft wing span.
B	Span of “flat plate” used to estimate intensity of flow field.
c	Wing chord.
C_l	Roll moment coefficient.
C_L	Non-dimensional wing lift coefficient.
$C_{l\alpha}$	Change in lift coefficient with angle of attack for 2-D analysis.
$C_{L\alpha}$	Change in lift coefficient with angle of attack for 3-D analysis.
C_{Lv}	Lift coefficient due to vortex.
I_{XX}	Roll moment of inertia.
g	Gravitational acceleration.
L	Lift.
m	Aircraft mass.
p	Aircraft roll rate.
$\hat{p}$	Non-dimensional roll rate.
q	Dynamic pressure.
r	Radius from wake core position.
R	Roll moment.
s	Radius from aircraft longitudinal axis.
S	Aircraft wing area.
Tc	Pilot delay time, from wake encounter to control input.
V	Wake vortex tangential velocity.
V_a	Airplane true airspeed.
V_c	Wake tangential velocity at the core radius.
V_{ref}	Airplane reference approach speed.
U_w	Upwash velocity on the wing due to the wake.
α	Angle of attack.
Γ	Wake circulation.
Γ_c	Wake circulation at the core radius.
Γ_S	Sensed wake circulation.
Γ_∞	Wake circulation at an infinite distance from the core for an isolated-wake vortex model.
$\hat{\Gamma}$	Wake average circulation.
λ	Wing taper ratio.
ϕ	Aircraft bank angle.
ρ	atmospheric density.
θ	Angular coordinate about the wake longitudinal axis.

Subscripts:

F	Refers to the Follower aircraft, the aircraft encountering a wake.
G	Refers to the Generator aircraft, the aircraft producing a wake.

Limitations of Current Vortex Strength Parameters

Past research on wake vortices have used numerous simplifying assumption in converting measurements to a circulation value. These assumptions can create significant differences from the circulation that would be determined from integration of vorticity in the wake region. These assumptions include the use of idealized wake velocity profiles, or models, that may not represent the actual flow as the wake decays, and ignores the effect of the ground and the nearby partner wake on measurements. The application of varying definitions of circulation by different disciplines or teams can result in confusion and results that cannot be directly compared. A second difficulty in determining circulation is that no known remote sensor technology can actually measure the circulation in any region of a free vortex in the atmosphere. Circulation estimates require either costly arrays of sensors to provide multiple lines of sight, or viewing angles, to a region in space or applying model assumptions to single-sensor measurements. Circulation measurements would require mapping the vector flow field. Doppler based systems in use can only observe line of sight velocity components. Assumptions and model fits used to estimate circulation from such measurements can work reasonably well when carefully applied by experienced wake observers to selected subsets of measurements. These estimates generally require examination of the data at hand to find measurement radii that best fit the expected circulation values for a particular size or type of wake generating aircraft.

Four wake vortex analytical models have been frequently applied to wake vortex studies in the past. These are the Lamb vortex (reference 3), the Hallock-Burnham vortex (reference 4), the Combined Rankine model, and the Hoffman-Joubert model (reference 5). The model equations are given in Appendix A. These models approximate tangential velocity profiles for an isolated vortex observed in laboratory or field studies. They are computationally simple to use, and can be used to initialize numeric wake simulations or perform aircraft/wake interaction studies. By specifying the location, core radius, and peak tangential velocity (or total circulation), an entire 2-dimensional flow field can be specified. With all models except the Hoffman-Joubert model, the flow field can be specified by computing the initial wake strength left by an aircraft and setting this value equal to the limit of model circulation as radius approaches infinity (total circulation). Figures 1 and 2 show the velocity profile and instantaneous circulation profile of each model as a function of radius. The core radius of each model was set to 1 meter and the model circulation was set to 200 $meters^2$/second. Direct application of these models is difficult in field studies since no known sensor can operationally measure the core radius or core velocity. Most measurements rely on model fits to estimate core size (reference 6). The resulting core size can vary greatly depending on the model chosen. For example, examination of figure 1 suggests that fitting the Hoffman-Joubert model to a wake velocity observation would result in a much smaller estimated core size than would be the case using any of the other three models.

Unfortunately decay is frequently modeled (in aircraft encounter studies or potential flow wake predictive algorithms) by assuming the velocity profile remains the same while the model circulation changes. Both ongoing CFD studies (references 7, 8, 9) and wake observations (references 10 and 11) provide evidence that the wake velocity profiles change during the decay process. In fact the authors of reference 11 are careful to refer to circulation profiles, rather than use the term circulation without qualification. Different decay rates at different radii from the core prevents the velocity profile from being described by a single circulation value. Reference 11 also discusses difficulties with using total circulation as a strength measure.

Use of a model based approach, where equal decay at all radii is assumed, may have several negative consequences. Fitting wake vortex field data from a decayed wake to a model profile that is no longer appropriate may produce misleading values of core size and circulation. Modeling the response of

aircraft to weak wakes, the fixed-profile assumption will provide excessive rolling moments at large wing span stations (assuming the wake tails have decayed faster than the core). When a fixed-profile vortex assumption is carried into any of various potential flow wake behavior models (references 12, 13, 14), the possibility of modeling wakes that stop sinking or bounce while retaining some strength is negated. For example the wake transport and decay model of reference 12 has been interpreted to indicate that a "bouncing" or rising wake has reversed its sign of circulation, yet flight data (reference 15) and ground based lidar observation efforts (references 16 and 17) indicate that wakes do rise without changing the sign of rotation. To construct more realistic transport models the modeler must introduce some number of additional, secondary vortices to steer the primary wakes (reference 13). This technique is not unrealistic, as CFD models and observations also show the creation of secondary vortices, but does not meet the need for an AVOSS strength definition for application to sensor observable characteristics. In fact, the process of defining the flow field becomes more difficult due to the need to know the position, core radius, and strength of multiple interacting vortices.

Although the use of simple analytical wake models has been and will continue to be valuable for various wake studies, a practical definition of strength, that does not depend on a particular velocity profile nor require core measurements, is required for the AVOSS system. This strength definition is required to coordinate the actions of various teams developing sensors, aircraft/wake interaction models, and decay prediction, as well as provide a parameter that can be used within AVOSS for application to reduced separations in safety-critical, revenue aircraft operations. The strength definition may be as simple as standardizing the radii over which velocity measurements will be processed, or may be more complex.

As mentioned above, different measurements of circulation may be obtained from flow fields or sensor observations. A primary factor affecting the measurements is the difference between the circulation, as obtained from integration of vorticity in a region, and estimated circulation from line of sight measures. This effect is particularly pronounced in a two-vortex system when the line of sight velocities are attributed to the wake being measured. The circulation at any radius from the core is found by integrating the tangential component, V(r), along a circle at that radius:

$$\Gamma(r) = \int_0^{2\pi} rV(r,\theta)d\theta \qquad (1)$$

While the sensed circulation at that radius, for an ideal line-of-sight remote sensor or array of in situ sensors applying an isolated vortex assumption is simply:

$$\Gamma_S(r) = 2\pi r\hat{V}(r) \qquad (2)$$

at that radius, where $\hat{V}$ is the average of the velocities measured on each side of the vortex core. Figures 3 and 4 show the geometry used in both calculations. Averaging the velocity from both sides of the core is typically done while computing strength from field data in order to reduce the effects of vortex drift and sink rate. Wake drift and sink may appear to add velocities to one side of the vortex while subtracting from the other side. Figure 3 shows the sensed velocity at r = 10 meters on the left and right side of a wake core as observed from directly below. The average of these two values would be used to compute the sensed circulation at radius = 10 of the left wake. The circulation of the region about the left core, however, would require integrating tangential velocities along a circle about the left core, as described by equation 1 and shown by the dashed line at radius = A in figure 4.

Equations 1 and 2 produce the same results only in the presence of axially symmetric flow, which is not the general case. A significant contribution to differences is the contribution of the partner vortex, which contributes additional downflow in the region between the two vortices while, to a much lesser extent, reduces the upflow in the region to the side of the vortex pair. As the radius from the vortex being sensed grows toward the distance separating the two vortices, very large velocities will be measured due to the second wake. When attributed to the wake being sensed, as will happen when equation 2 is implemented in a practical sensor, these high velocities create a high circulation estimate.

The above values are considered "instantaneous" circulation values, as they represent the circulation at a particular radius from the core. In practice an "average" circulation value is normally computed

to make use of more data and reduce the effect of measurement noise and atmospheric turbulence. The average circulation makes use of all computed circulation values between any two radii, making use of the velocities on both sides of the core. The average circulation is simply:

$$\hat{\Gamma}_{a,b} = \frac{1}{b-a}\int_{a}^{b}\Gamma(r)dr \qquad (3)$$

where $\Gamma(r)$ is the sensed instantaneous circulation from equation 2 for field data or the true circulation value from equation 1 for diagnosed data from numeric or analytical models. The shaded area in figure 4 represents the region of integration for the true circulation about the left wake, while the velocities normal to the observational slice through the wake, between radius = A and radius = B, represent the data that would be used to compute a sensed circulation.

Although equation 3 is strictly only correct for an isolated vortex, field measurement limitations create situations where it is commonly applied to two-vortex situations. Uncertainty as to the location of the partner vortex limits the opportunity for corrections, and care is typically exercised by researchers to choose averaging radii that minimizes error. Dr. Rick Heinricks of MIT Lincoln Laboratory has derived an analytical expression (reference 17) for the difference between the wake circulation and the sensed average circulation. Figure 5 was produced by Dr. Heinricks and is reproduced from reference 17. This plot assumes a line of sight Doppler sensor located directly below the vortex pair and plots the theoretical overestimate of circulation for different averaging radii (a and b in equation 3) for various core separation distances. Vertical lines indicate the expected core spacing, out of ground effect, for several aircraft types. As can be seen, the circulation sensed from field measurements can be significantly greater than the individual vortex circulation.

As a more general illustration of the limitations for circulation estimates and model based approaches, equations 1 through 3 were coded at Langley to diagnose the average circulation and average sensed circulation for three of the wake models shown in figure 1. As is commonly done in field studies, two wakes were present in the model and contributing to the flow field while the equations for diagnosing circulation were applied to one of the vortices. The Combined Rankine data is not plotted since it is nearly identical to the Lamb vortex results. This code allowed the sensed circulation to be computed at any viewing angle, from vertical to horizontal, and any arbitrary vortex pair core spacing and altitude placement. A viewing angle of zero represents a vertical viewing angle and 90 degrees represents a horizontal view of the vortex. A perfect line of sight measurement is assumed and no sensor specific error sources or biases are modeled. For this illustration the core spacing was 36 meters, and the core radius was 2.3 meters. This is roughly representative of the wake dimensions from an aircraft of span 46 meters (150 feet). The total circulation value used to establish the wake model was arbitrarily set at 100 m^2/s. Since the circulation value in the Hoffman-Joubert model increases with increasing radius without limit, this model was arbitrarily initialized by assuming that the circulation at the core radius was the same as that for the Hallock-Burnham model, or one-half the total circulation.

Both the actual circulation from 5 to 10 meters radius and the sensed circulation between the same radii are shown for all viewing angles in figure 6. The wake circulation is not dependent on viewing angle while the sensed circulation is plotted as a function of viewing angle. The first obvious observation from the plot is that the different models produce different circulation values in a given region due to differing vorticity distributions. The true average circulation for the Lamb vortex in the 5 to 10 meter range was equal to the model input of 100 m^2/s, while the Hallock-Burnham model value was only 90.5 and the Hoffman-Joubert model value was 107. This emphasizes the fact that given a field measurement, the choice of model that is applied to that data may effect the interpretation of strength. Another observation from figure 6 is that the sensed circulation varies about 5% each side of the true circulation with changes in viewing angle. As shown by Heinricks (figure 5) this effect can be much greater (10% to 40%) at other core spacing and averaging intervals.

At this point multiple methods of determining circulation have been introduced. The circulation is related to the total impulse imparted on the atmosphere by a passing aircraft and the sensed circulation is a view of a subset of that atmospheric motion along a particular axis or line of sight. The sensed circulation differs from the actual

circulation in the same wake radii interval due to lack of symmetry of the actual flow field. The relationship between these values vary with the core radius, core spacing, circulation averaging radius and wake model (velocity profile) chosen for interpretation. Confusion can arise between the various disciplines involved in the AVOSS development when a value produced by one team, for example field data, is interpret by another team, for example aircraft/wake interaction or CFD model validation, as representing a different circulation value. For example a minimum detectable wake circulation by a field sensor of 100 m^2/s may be equivalent to a total, or model, circulation value of only 70 m^2/s for wake models being applied to aircraft response studies. Likewise field observations of wakes by the Lincoln lidar at Memphis were initially thought to be in error because the sensed circulation was frequently larger than the circulation values expected from the generating aircraft. The type of analysis conducted by Heinricks and discussed above showed the field measurements to agree quite well with theory when the difference between sensed circulation and actual circulation was considered.

The remainder of this report will attempt to present a method for standardizing the vortex strength definition for use within the AVOSS system. Within the context of this report and AVOSS design, the following terminology is used. The term "strength definition" refers to a method of quantifying the vortex flow field intensity. Examples include tangential velocities, circulation, and average circulation. The term "acceptable encounter definition" refers to the response of an aircraft to a wake encounter, in terms that can be discussed with the FAA, pilot community, and air transport operators. Examples include maximum bank angle, roll rates, fraction of control authority required to compensate, flight path deviation, or touchdown dispersion. By defining a strength definition that scales to candidate acceptable encounter definition parameters, and gaining industry consensus or concurrence on acceptable operational encounters, a threshold strength definition becomes available to AVOSS for use in subsystem design and in defining acceptable spacing.

AVOSS Vortex Strength Definition Requirements

Within the context of a wake vortex spacing system implementation, a primary requirement is to define a wake strength parameter that correlates to the operational impact of a wake encounter, can be used to guide the development of practical sensors, whose decay rate can be predicted as a function of initial wake and atmospheric conditions, and that can be diagnosed from numeric wake simulations. Preferably the strength definition should be represented by a single number, or a very limited set of numbers. For example, the average circulation taken over the scale length of the follower aircraft semi-span was considered as a candidate strength definition. This definition may not be feasible due to sensor inability to measure wake velocities at large radii from the core, would require a large set of strength definition values, and would possibly require AVOSS software or data base upgrades as new aircraft are introduced. If one or several values can be found that meets all subsystem requirements the AVOSS design will be simplified. The question that has not yet been answered, and that is being asked, is how to best quantify ideal line of sight observations in an automated system to describe vortex strength and aircraft response. Rather than asking "How do we estimate total circulation and core size from sensor observations" this effort will attempt to ask "How do we characterize velocity profiles to define a parameter that scales well with the effect on an encountering aircraft?" The strength definition will attempt to meet the following three subsystem characteristics.

1. Sensor Characteristics

AVOSS sensors may include some combination of Doppler Lidar, Doppler radar, ground wind lines (in situ anemometers) or other sensors. Currently the Lidar is the most mature remote sensor technology and has been in research use for decades for wake measurements. Doppler sensors are limited to measuring line of sight velocity components and cannot map the 2-dimensional flow field of a wake, without resorting to complex and costly multiple Doppler sensor techniques. Operational experience with Doppler lidar also suggests a limited range of vortex radii that can be measured. Discussions with Langley and Lincoln Lidar developers, experience with the lidar data sets collected at Memphis in 1994 and 1995 by Lincoln, and reference 11, suggest that velocity

measurements at scales less than the core radius are not reliable. Two factors prevent accurate measures of these velocities, (1) the size of the region where the velocities occur can be very small compared to the focal volume or pulse length of the Doppler system and (2) the signal to noise ratio can typically be very small in that region. Operational experience also suggests an outer limit to the radii for meaningful vortex measurements. At large radii the vortex velocities become small relative to atmospheric turbulent velocities, ambient wind and vertical shear, vortex drift rate, and sensor system noise. The Lincoln data set from Memphis frequently does not contain circulation values beyond 15 to 20 meters core radius. In comparison the semi-span of many heavy aircraft is on the order of 20 to over 30 meters.

Another assumed sensor characteristic derives from the AVOSS requirement to monitor wake behavior beyond the airport boundary, possibly to distances of 2 or more miles from the runway. Practical siting constraints at most airports, combined with potential minimum and maximum range characteristics of various sensors, may require arbitrary viewing angles. For example the NASA Langley Doppler Lidar has a minimum range of approximately 800 meters and must be sited to the side of the approach path. Additionally the strength definition should assume that the sensor does not have knowledge of the generating aircraft type, the follower type, and may not be able to track both vortices at the same time. Potentially, a vortex may depart the sensor volume while the other stalls in the localizer region.

The strength definition investigation will make use of the assumptions above but will not attempt to accommodate sensor specific characteristics such as velocity averaging over pulse lengths or the influence on velocity measurements due to other vortices in the line of sight but away from the focal volume (for continuous wave systems). The assumption is made that ideal line of sight measurements can be made, but only within a limited range of core radii.

2. Wake Geometry Characteristics

The AVOSS strength definition should not strictly depend on any assumed spacing or relationship between the vortex cores. Much basic wake research into aircraft encounters assumes the elliptical loading based core spacing of $\pi/4$ of the generator wing span, and equal sink rate of both wakes in the vortex pair. Although this case is frequently observed, particularly early in the wake lifetime, it does not represent the general case. Vortex proximity to the ground cases the separation to increase and cross wind shear conditions are known to cause unequal wake sink rates. Also, as mentioned above, there may be situations where operational sensors can only track one vortex. Since AVOSS is intended to work in ground effect and in most weather conditions the general case of arbitrary vortex locations will be assumed.

3. Aircraft/Wake Interaction Characteristics

The strength definition must scale to the operational impact of an encounter by following aircraft. A significant effort is underway within Langley, in conjunction with the FAA and industry, to define wake interaction with aircraft and set acceptable encounter thresholds (references 18 and 19). Factors being considered include bank angle response, induced roll rates, fraction of control authority required to compensate, flight path deviation, touchdown dispersion, and pilot and passenger acceptance. While the results of this research will be used to develop industry consensus, determine whether decay can in fact be used by AVOSS as a separation reducing factor, and set system thresholds, these results may not be available for several years. A vortex strength definition and initial threshold estimates are required now to interpret field data, develop sensors, and conduct initial AVOSS system trades. Using earlier research conducted at Ames Research Center (reference 20), an assumption will be made that quantifying the maximum bank angle achieved in a sudden encounter, using a reasonable aircraft and pilot model, will enable development of a strength definition, and eventually threshold values, that will be reasonably close to the final results of the more rigorous hazard definition work. Although no attempt will be made to set threshold values in this paper, the hypothesis is made that finding wake strength values that produce negligible bank angle changes, while the aircraft is being controlled by a pilot model limited to about 1/4 to 1/3 roll control authority, will produce thresholds representative of those that may possibly be used within AVOSS. These bank responses are believed to be typical of those frequently experienced in low altitude turbulence,

and must not interfere with normal localizer tracking.

Analysis Technique

The analysis presented here represents only a first approximation to the establishment of a suitable strength definition. The general approach is to create an array of wake vortex scenarios, representative of the wakes that may be created by an assortment of aircraft types, diagnose the strength of each wake using multiple candidate strength definitions, model the bank angle response to an array of encountering aircraft caused by each wake scenario, then determine which measure of strength best correlated to the responses.

Five lead aircraft were modeled. These were the DC-9-50, Boeing 727-100, Boeing 767-300, DC-10-30, and Boeing 747-400. The intent was to provide wake characteristics representative of a wide range of transports, with some bias toward the heavier aircraft. To further vary the wake encounter scenarios two wake strengths were used. For each generator aircraft, the theoretical initial wake strength and one-half that strength were used to specify the wake profiles for the 3-DOF encounter model. Wing span was multiplied by $\pi/4$ to determine the default core spacing. A spacing of infinity was also simulated to bound the effects of greater than default wake spacing. An aircraft approach weight of about 75% of the maximum certified landing weight was used. The Hallock-Burnham wake vortex model was used to represent the generated wake, and the core size was chosen to be 5% of the span of the generator. Table 1 lists the characteristics of each generating aircraft and wake scenario. Although 5 scenarios are shown, the use of two core spacings, two viewing angles, and two strength values per aircraft resulted in 40 scenarios per following aircraft type being modeled.

Four follower aircraft were modeled. These were the Jetstream Super 31 (a twin-turboprop commuter), the Boeing 737-200, Boeing 727-100, and DC-10-30. These aircraft were intended to represent a wide range of encounter aircraft, with some bias toward the smaller aircraft.

Candidate Strength Definitions

Three candidate strength definitions and a baseline metric were computed for each of the 40 wake vortex scenarios. The candidate strength definitions are average sensed circulation, calculated torque on a flat plate, and the maximum tangential velocity of the wake. The baseline metric is the total circulation shown in table 1 and used to specify the wake models. The first two strength definitions were computed for a number of variations of spatial intervals. When combined with the total circulation value and the maximum tangential velocity value, a total of 14 wake strength values were determined for each encounter scenarios.

Eight strength values were derived for the sensed average circulation definition by computing for 8 different average intervals. The intervals chosen were 1 to 5, 1 to 10, 1 to 15, 3 to 10, 5 to 10, 5 to 15, 7 to 15, and 10 to 15 meters. These limits correspond to the limits a and b in equation 3. The intent was to avoid using core measurements or measurements beyond 15 meters radii and to select a number of different radii limits to vary the emphasis from near core to other portions of the wake velocity profile. These 8 strength values were computed for both vertical viewing angles to the wakes (viewing angle of zero) and a nearly horizontal look at the vortex (viewing angle of 80 degrees). This varies the sensed strength value according to the effect described by figure 6.

Four strength values were computed for the flat plate torque definition. This parameter was based

Table 1: Generating aircraft and initial wake specifications:

Case #	Aircraft	Weight, kg.	Vref, m/s	Span, m	Core Spacing, m	Core Radius, m	Total Circulation, m^2/s
1	DC-9-50	37422	68.0	28.48	22.36	1.42	197.03
2	B727-100	45927	70.0	32.93	25.85	1.65	227.26
3	B767-300	94575	70.0	47.59	37.37	2.38	289.84
4	DC-10-30	137100	71.0	50.43	39.59	2.52	387.66
5	B747-400	214325	74.6	64.33	50.51	3.22	431.75

on a concept originally proposed by Dr. Roland Bowles of Langley, to estimate the torque on a flat plat immersed within the flow. The derivation of this strength definition, called H, is presented in Appendix B and is given as:

$$H(B) = \int_{-B/2}^{B/2} \left[1 - \frac{2|s|(1-\lambda)}{B} \right] V(s) s ds \qquad (4)$$

where the term in square brackets is the wing chord and is computed from the taper ratio of the flat plate (λ), the span of the plate (B), and the position along that span (s). The factor H may be computed for plates, representing a wing, at different scale lengths. Four scale lengths, 10, 20, 30 and 40 meters, were chosen. The taper ratio for these lengths were set at 1.0, 1.0, 0.5, and 0.3 respectively. The data used to choose these values is shown in Appendix B and is intended to represent typical wing chord taper ratios of transport aircraft within different wing span groupings. Note that the parameter H(B) is very similar to circulation, with the addition of the wing chord weighting function. A significant difference in H(B) is the inclusion of the core region as the integration is carried from -B/2 to B/2. This was due to the fact that the H(B) parameter was derived prior to the field experience and other sensor development activities that suggest core measurements and large radii velocities are not reliably available. This initial analysis of various strength definitions was conducted with the originally derived H(B) parameter and follow on analysis is needed to evaluate its performance using the same radius restrictions as the average circulation parameters.

Aircraft-Wake Encounter Model

The aircraft wake encounter model is the result of work described in reference 21. This code provides a 3 degree-of-freedom (DOF) model of an aircraft interacting with a wake pair, including vertical and lateral translation. A simple pilot model provides a fixed delay between the wake vortex entry and the application of roll control to alleviate the wake. For the runs presented in this report the pilot delay was 0.60 seconds and thereafter full roll control authority was provided. These conditions replicate the technique used in reference 21. The model is capable of Monte-Carlo determination of the worst-case wake entry point, which is not always at a core location, and the worst case location was used in this effort. The values to be presented are the maximum bank angles reached during each simulated encounter. Details of the aircraft/wake encounter model are presented in reference 21 and summarized in Appendix C.

Relative Weighting of Vortex Radius

Another, independent approach to assess the most critical wake radii with respect to aircraft reaction was performed as follows. A dual wake vortex pair was modeled with the Hallock-Burnham wake model. The wake flow field was then subjected to a 1-meter wide notch filter that let through only the computed velocities within the range of radii included in the filter. The filter could be moved to any radius from the left vortex core. A set of representative aircraft were imposed at the left core position and the resulting quasi-steady roll rate was estimated as the position of the notch filter was moved from the left aircraft wing tip to the right wing tip. The specified position of the notch filter is the filter mid-point. For example a notch position of 5 meters indicated that wake velocities from 4.5 to 5.5 meters are passed and the wake velocity at all other radii is zero. The wake radii is the same value as the wing span location since the aircraft is centered in the core. The resulting roll rates can be used to assess the range of wake radii most significant to each aircraft.

The following assumptions are used in the analysis. Only a wing was modeled for the follower aircraft. No fuselage or tail surfaces were included. A constant span-wise Cl_α was assumed for each aircraft with the wing mid-span point located at the center of the core of the left wake. The wake vortex pair was assumed to have a core radius of 2 meters and a core spacing of 30 meters. This is roughly representative of a wake generated by an aircraft of 38 meters span if a core radius of 5% of the generator span and a core spacing of $\pi/4$ of the generator span is assumed. The cores are assumed to be located at identical altitudes and the model total circulation is arbitrarily set at 200 m^2/s. No perturbation of the wake by the encountering aircraft is modeled, such as the wake being deflected by a fuselage, and no corrective roll control inputs are modeled. The wake velocity is simply allowed to impinge on a 1-meter strip of the wing's span and the roll rate required for natural damping (total roll moment equal to zero) is computed. This rate is considered quasi-steady since the roll motion would change the relationship

between the wing and the wake pair flow field as would aircraft vertical and lateral motion induced by the roll. In this analysis the aircraft wing is not allowed to change position or bank angle. The intent is not to accuracy model a particular aircraft encounter with a wake, but to determine the relative weighting along the span for the effects of the wake on the aircraft reaction. The equations used to estimate roll moment and rate are.

$$R = \int_{-b/2}^{b/2} \Delta L(r) r dr \qquad (5)$$

where ΔL is the section lift change induced by the wake or the roll rate and r is the distance from the wing mid-span point.

$$L = \frac{1}{2}\rho V^2 S C_L \qquad (6)$$

where ρ is air density, V is the airspeed of the follower aircraft, S is wing area and C_L is the wing lift coefficient. The change of lift at any span section is:

$$\Delta L = \frac{1}{2}\rho V^2 C l_\alpha \Delta\alpha(r) c(r) dr \qquad (7)$$

where c(r) is the wing chord at span r, S has become c(r)*dr*, and the change in Cl is Clα multiplied by the change in local angle of attack at the span location r. The change in local angle of attack is a function both of the wake and the induced upwash from the roll rate.

$$\Delta\alpha(r) = \frac{U_w(r)}{V} + \frac{r\dot{\phi}}{V} \qquad (8)$$

where $U_w(r)$ is the upwash from the wake vortex at span location r, and ϕ dot is roll rate. Combining equations 5 through 8 gives the roll moment.

$$R = \frac{1}{2}\rho V C l_\alpha \int_{-b/2}^{b/2} (U_w(r) + r\dot{\phi}) c(r) dr \qquad (9)$$

For each location of the notch filter the wake velocity was computed along the span, then the roll rate required to produce a zero rolling moment was determined. Note that the wake is only acting along a 1-meter wide portion of the wing span while the roll damping acts along the entire span. The computation was performed numerically using 10 span-wise points per meter. There is no need to know $C_{l\alpha}$, ρ, or airspeed since the roll moment is being set to zero. Only the follower aircraft span and taper ratio is required to determine the roll rate required to null the forces.

A range of encountering aircraft sizes was considered, from a very short wing-span commuter to the largest wing-span commercial transport. The inputs to the model were intended to be representative of the encountering aircraft shown in table 2.

Table 2 - Encountering Aircraft Specifications for Relative Roll Rate Calculation.

Aircraft	Span (m)	Taper Ratio
BaE31	15.9	0.38
DC9-50	28.5	0.24
B737-200	28.4	0.34
B727-100	32.9	0.30
B757-200	38.0	0.23
B767-300	47.6	0.27
DC10-30	50.4	0.25
B747-400	64.0	0.25

Results

Simulation Data and Correlations

Table 3 shows the 14 strength definition values for each of the 20 full strength wake vortex scenarios. Cases 21 through 40 duplicate cases 1 through 20, in the same order, with the exception that the wake model total circulation and all strength definition values are one-half of those indicated in this table. Note that in the case of infinite core spacing the strength definitions do not vary with viewing angle. The column labels beginning with C indicate average sensed circulation at the indicated radius limits, the labels beginning with H indicate the H(B) index at the indicated plate span, and Vc indicates the vortex model peak tangential velocity.

Table 4 shows the maximum aircraft bank angles, in degrees, as determined from the encounter model for the same 20 encounter scenarios plus the 20 one-half strength wakes. The first 4 data columns indicate the response for the full strength vortices and the last four columns contain the bank angles for the one-half strength vortices. Note that in most cases a wake strength of one-half the initial strength produces much less than one-half the roll response, due to non-linearities in the encounter such as the roll induced during the period that the pilot input is being delayed.

As a first look at the ability of each strength definition to describe aircraft response, the data in these tables were subjected to simple linear regression techniques. The coefficient of determination was examined for each regression fit to identify strength values that correlated well to response. For each strength value the linear regressions were performed individually for each of the four follower aircraft types. The means and standard deviations of the regression coefficient of determination were then determined. A low standard deviation indicates that the regression coefficient of determination was nearly equal for each aircraft type while a high standard deviation indicates that the coefficient of determination varied greatly between aircraft types. Various combinations or grouping of the data was made to examine correlations for all situations and singly for specific cases such as vertical viewing angles. Figure 7 shows the mean and standard deviation of the coefficient of determination for all of the aircraft encounter data, including all viewing angles, both core spacing values, and both full and one-half strength wakes. The strength definitions on the horizontal axis are sorted in decreasing order of the mean coefficient of determination. This plot suggests that most of the average sensed circulation values correlated to bank response essentially as well as the total circulation value used to specify the wake models, both in terms of the average coefficient of determination and in the variation between aircraft. There is no apparent advantage of the H(B) factors over the average circulation factors, and the maximum core velocity correlated much worse that any of the other values.

Figures 8 and 9 show the same data, only now grouped separately into all full strength wake encounters and all one-half strength encounters. The results are similar except that more discrimination between the various strength parameters is shown. In all three figures the 5 to 10 meter average sensed circulation comes very close to matching the performance of the model input circulation. Circulation averages and H(B) factors that emphasize the region near the core (the 1 to 5 meter average circulation and the H(10) factor) or the extreme outer region (10 to 15 meter average circulation or H(40) factor) perform poorly compared to the model input circulation, while the core velocity essentially does not correlate with bank response. The core velocity will be dropped from the remaining analysis.

Figures 10 and 11 show the coefficient of determination of the remaining 13 strength definitions grouped by viewing angle. Both core spacing values are represented in this data. Figures 12 and 13 group the statistics by core separation while including both viewing angles on each plot. Only the full strength vortex encounters are represented on these four plots. These data also suggest that parameters that weigh the extreme inner or outer regions of the wake correlate poorly compared to a more central region, from about 5 to 15 meters. While more complete analysis is needed to arrive at a final AVOSS system strength definition, the results shown above lead to the preliminary suggestion to use the sensed 5 to 10 meter average circulation to quantify wake strength. The relative insensitivity of the coefficient of determination to other similar radii, such as 7 to 10 meters or 5 to 15 meters, suggests significant flexibility for sensor designers. For example additional data points could be collected for signal processing by using the larger 5 to 15 meter interval.

Table 3 - Strength Definition Values for all Full-Strength Wake Scenarios

Case #	Lead Aircraft	Viewing Angle (deg)	Spacing	Total Circulation (m^2/s)	C5-10 (m^2/s)	C10-15	C7-15	C5-15	C1-5	C1-10	C3-10	C1-15	H(10) (m^3/s)	H(20)	H(30)	H(40)	Vc (m/s)
1	DC9	0	default	197.03	216.8	291.9	268.2	255.4	147.7	184.6	206	223.6	203.7	547.7	714.6	1068.8	11.012
2	B727	0	default	227.26	238.2	297.2	279.1	268.2	158.4	200.7	225.9	235.2	216.8	594.9	750.3	1060.1	10.985
3	B767	0	default	289.84	273.3	317.6	305.2	295.3	161.8	220.7	254.9	254.3	216.7	651.8	810.5	1018.5	9.6928
4	DC10	0	default	387.66	359.4	416.9	401.1	387.8	207.7	287.9	333.8	332.5	277	849.3	1058.1	1326.8	12.235
5	B747	0	default	431.75	368.8	433.4	416.5	400.3	189.1	284.7	335.5	335.8	247.5	835.2	1058.1	1327.4	10.682
6	DC9	80	default	197.03	169.2	147.8	154.9	158.3	139.1	153.7	167.8	150.9	193.6	464.3	515.8	582.7	11.012
7	B727	80	default	227.26	197.6	180.6	186.5	188.8	150.9	174.3	193.4	175.6	208.1	524	592.3	677.9	10.985
8	B767	80	default	289.84	248.9	250.6	251.7	249.2	157.3	204.8	235.3	219.7	211.4	609.1	719.3	849.8	9.6928
9	DC10	80	default	387.66	330.4	337.4	337.5	333.1	202.3	268.9	310.5	291.4	270.7	798.4	949.8	1127.6	12.235
10	B747	80	default	431.75	348.9	379.7	373.5	363.2	185.4	271.8	319.5	308	243.1	800.6	984.6	1193.9	10.682
11	DC9	0	infinity	197.03	189.2	194.4	193.3	191.7	143.1	166.8	184	176.1	198.3	499.8	584	693.4	11.012
12	B727	0	infinity	227.26	215.3	223.2	221.5	219.1	154.4	185.9	207.7	198.5	212.3	555.4	653.9	779.9	10.985
13	B767	0	infinity	289.84	260.2	279.4	275	269.4	159.5	212.2	244.4	234.9	213.9	629	759.8	919.5	9.6928
14	DC10	0	infinity	387.66	343.9	372.1	365.5	357.3	204.9	277.8	321.4	309.7	273.7	822.3	998.4	1211.6	12.235
15	B747	0	infinity	431.75	358.3	404.2	393.2	380.3	187.2	277.9	327.1	320.8	245.2	817.1	1018.7	1253.7	10.682
16	DC9	80	infinity	197.03	189.2	194.4	193.3	191.7	143.1	166.8	184	176.1	198.3	499.8	584	693.4	11.012
17	B727	80	infinity	227.26	215.3	223.2	221.5	219.1	154.4	185.9	207.7	198.5	212.3	555.4	653.9	779.9	10.985
18	B767	80	infinity	289.84	260.2	279.4	275	269.4	159.5	212.2	244.4	234.9	213.9	629	759.8	919.5	9.6928
19	DC10	80	infinity	387.66	343.9	372.1	365.5	357.3	204.9	277.8	321.4	309.7	273.7	822.3	998.4	1211.6	12.235
20	B747	80	infinity	431.75	358.3	404.2	393.2	380.3	187.2	277.9	327.1	320.8	245.2	817.1	1018.7	1253.7	10.682

Table 4 - Aircraft Bank Angle Response (degrees) for 40 Wake Encounter Cases

Case #	Super 31	B737	B727	DC10	Case #	Super 31	B737	B727	DC10
1	55.3	27.5	18.9	9.3	21	24.32	9.18	7.1	2.4
2	61.1	32.2	28.3	12.0	22	28.15	10.76	9.27	3.18
3	68.5	40.0	36.0	15.0	23	32.76	13.59	11.54	3.28
4	87.4	54.0	49.3	23.7	24	45.34	22.25	19.39	6.13
5	87.0	56.5	52.2	26.4	25	44.43	23.37	20.6	6.36
6	55.3	27.5	18.9	9.3	26	24.32	9.18	7.1	2.4
7	61.1	32.2	28.3	12.0	27	28.15	10.76	9.27	3.18
8	68.5	40.0	36.0	15.0	28	32.76	13.59	11.54	3.28
9	87.4	54.0	49.3	23.7	29	45.34	22.25	19.39	6.13
10	87.0	56.5	52.2	26.4	30	44.43	23.37	20.6	6.36
11	58.7	26.2	22.2	5.3	31	23.82	7.08	5.63	1.22
12	65.4	31.9	27.6	7.4	32	28.16	8.9	7.12	1.54
13	73.5	40.9	36.7	12.6	33	33.33	12.49	10.24	2.26
14	100.8	56.8	52.2	23.2	34	46.78	21.48	18.32	4.38
15	97.5	59.1	55.0	26.4	35	45.7	23.05	20.09	5.19
16	58.7	26.2	22.2	5.3	36	23.82	7.08	5.63	1.22
17	65.4	31.9	27.6	7.4	37	28.16	8.9	7.12	1.54
18	73.5	40.9	36.7	12.6	38	33.33	12.49	10.24	2.26
19	100.8	56.8	52.2	23.2	39	46.78	21.48	18.32	4.38
20	97.5	59.1	55.0	26.4	40	45.7	23.05	20.09	5.19

Although the strength definitions were diagnosed without consideration of sensor specific characteristics, by assuming ideal line of sight measurements, the strength parameter that seems to correlate best with aircraft bank response also happens to rely on that portion of the vortex that is likely to be most easily quantified by practical sensors. Qualitatively this result can be explained as follows. Vortex velocities near the cores are relatively invariant with viewing angle, but do not adequately describe the rolling moment induced on the wing of any but the smallest of following aircraft. Although velocities may be high in this region the induced velocities on a following wing occur over too small a portion of the span to have a great effect. At very large radii the sensed strength of the wake becomes very sensitive to the observation viewing angle, while the aircraft response has no dependency on the sensor view angle. The velocities that are measured at the larger radii are in most cases very small. These small velocities, at large span stations on a wing, can only induce very low roll rates, even if the wing were to perfectly follow the tangential flow at that station. There appears to be a region within the vortex where the velocities are substantial, the sensed strength is relatively insensitive to viewing angle, and where the span wise position on a following wing is suitable to induce significant roll rates.

Predicting Roll Response

In an effort to derive an expression to predict the actual roll response of following aircraft, the data in tables 3 and 4 was subjected to regression techniques. For the full strength wake encounters the bank angle was found to be almost linear with respect to the product of the 5 to 10 meter sensed circulation and the log of the follower aircraft span or weight. Figure 14 shows the relationship between the response and the log of follower span (on the left Y-axis) and follower weight (on the right Y-axis). The weight plotted in this figure is the certified maximum landing weight of the aircraft, not the actual weight used in the simulation. The term “slope” in figure 14 is equivalent to the term in parenthesis in equation 10 below.

The relationship between the follower aircraft span and bank response can be expressed for these full strength wake encounters by:

$$\phi_{\max} = \hat{\Gamma}_{5,10}(0.768953 - 0.41637\log(span)) \quad (10)$$

When the results of this equation were compared to the aircraft simulation model output for all the full strength encounters, the difference between equation 10 and the 3-DOF model bank angle responses rarely exceeded 10 degrees, even for cases where the smallest aircraft was reaching bank angles in excess of 90 degrees. Unfortunately, equation 10 provided a poor prediction of aircraft response when compared to the 3-DOF model response to the encounter scenarios that used 1/2 strength wakes. In many cases the bank predicted by equation 10 was far greater than the modeled response. This is likely due to the strong non-linear characteristics of the wake encounters, such as a fixed pilot reaction delay that is not dependent on the wake strength. The inability of the equation to predict bank angles with weaker wakes also means that it cannot be used to estimate the wake strength that would be required to produce a small but acceptable aircraft bank angle change. This inability to predict low response values with data obtained with high response angles also suggests that the data set computed above and shown in tables 3 and 4 should be computed at a fixed bank response angle for each aircraft rather than for a fixed wake strength.

Relative Weighting of Vortex Radius

Figure 15 shows the results of the analysis of aircraft roll rate caused by a wake subjected to a notch filter. The computed quasi-steady roll rate for each of the 8 aircraft is shown. As expected, the smallest aircraft experienced a much greater roll rate than any of the jet transport aircraft. The largest aircraft, those whose semi-span begins to approach the core of the right wake, experienced maximum induced roll rates when the notch filter was moved near the right wake core. The B-747 was the only aircraft whose wing tip actually reached beyond the right core. As the notch was moved into and through that core the peak roll rate was found. A rapid reversal in roll direction was seen when the notch was moved to the opposite side of the right core. It should be pointed out that this effect depends to the equal altitude of the two cores. The effect would be largely self-alleviating in an actual encounter as the aircraft begins to roll and the wing tip moves way from the wake core. The higher roll rates seen by the smaller aircraft would not be self alleviating as would the roll effect on the larger aircraft. The flow field would alter only slightly as bank angle increases, until aircraft lateral or vertical motion moves the wing away from the wake. For all other aircraft, of B-757 size and below, the peak roll rate falls in the 4 to 5 meter notch position.

The asymmetry of roll rate between the left and right side of the aircraft is due to the asymmetry of the 2-vortex flow field. The wake velocities are higher between the wake cores than outside the two cores. The relative roll rates on the left side of the aircraft mid-span are a close approximation to the results that would be seen with only a single vortex. This data has been normalized with respect to the maximum roll rate of each aircraft type and plotted in figure 16. This plot shows a remarkable similarity between the aircraft types in terms of the radii of greatest wake influence. Every aircraft showed the greatest effect from that portion of the wake between 4 meters and 5 meters. This location is at more than twice the wake core radius. The roll effect at the core radius is about 70% of the maximum effect. In reality the effect at the core radius would be less due to the effect of the fuselage. The effect of the wake drops rapidly with increasing radius beyond 5 to 6 meters, such that the relative effect is below 70% at 15 meters for even the largest aircraft and below 45% at 15 meters for all the large and small category aircraft modeled.

While this analysis does not establish an obvious strength definition, it does suggest a bound to the problem and corroborates the results seen by the statistical processes. This analysis in no way assumed any sensor characteristics. The analysis only suggests the most significant wake region to include in strength quantification. Wake radii below 4 to 5 meters appear to be much less significant than a region bounded by a minimum of 4 to 5 meters and a maximum of 10 to 20 meters. Many of the aircraft have semi-spans of less than about 15 meters and would therefore be unaffected by the larger radii. Even the largest aircraft experiences almost one-half the cumulative effect (the relative area below the curve) below 15 meters radius and the other two heavy aircraft experienced about ¾ of their cumulative effect below 15 meters. The analysis suggests that, if one

quantification scheme were to be employed to define strength for the entire fleet, within an AVOSS system, the range of radii chosen should be bounded at the low end by values of 4 to 5 meters and at the high end by values of 10 to 15 meters. Smaller radii would represent little influence on the aircraft and larger radii would quantify the wake in regions of no significance to the lower wing span aircraft. If multiple strength quantification's were employed within AVOSS, the definition above could be applied to small and large aircraft, and a larger radius on the order of 5 to 25 meters could be applied to the heavy aircraft category.

Additional studies could be performed to reevaluate these conclusions with different wake core spacing and core sizes and with different encounter geometry. For example, would there be an advantage to the quantification of larger radii for the case of an aircraft encounter at a point between the cores rather than centered on a core? In performing any such analysis the AVOSS system requirements must be considered. There are no wake vortex constraints to ATC-applied spacing for any aircraft behind a small aircraft or for large aircraft behind other large aircraft. Runway occupancy considerations limit aircraft spacing for these pairs rather than the wake. Quantification of the wakes generated by small aircraft is not required for AVOSS and any quantification of large aircraft wakes should be biased towards improved accuracy for the smaller aircraft. Accurate quantification of heavy aircraft wakes is required for all classes of following aircraft.

Additional Work Required

The model results and data shown above represent only a preliminary attempt to establish a strength definition suitable for application to the AVOSS. Additional effort is required to address several areas. First, the aircraft/wake encounter simulation should be rerun with more aircraft types, more wake scenarios, and with different wake analytical models. The different wake models should include both variations in the core size assumptions for the models used as well as choosing models with different vorticity distributions. Since one desired characteristic of the suggested strength definition is that it is relatively insensitive to the wake velocity profile, the model needs to be run with alternate wake profiles. More detailed statistical analysis is also called for to determine the significance of the correlations and identify the dependencies of the various factors (e.g., wake core spacing, viewing angle) on the results. Finally, the wake interaction model should be run with each wake scenario, and with different wake model circulation values, to determine the strength required to produce a given response. The suggested first value for this analysis is 5 degrees of response, plus or minus one degree. This may require a large set of runs to be run to find the required strength for each scenario. The primary purpose of these runs is not to establish a final threshold strength for each aircraft for operational use, but to determine if the same parameter retains the best correlation to the data at the lower strength values. The resulting threshold values for each aircraft will also provide a "ballpark" number for initial AVOSS design decisions.

Future analysis should be conducted with a definition of the H(B) factor that is consistent with the criteria used to define the average circulation factors. Specifically the H(B) value should be computed without using information in the core region. Additionally, other concepts for strength definitions have been proposed at Langley. Time did not permit these to be evaluated in this initial analysis.

Concluding Remarks

An analysis was conducted to determine an appropriate wake vortex strength index for application to the NASA Aircraft Vortex Spacing System (AVOSS). The purpose of the strength definition is to provide a parameter that can be agreed to by multiple teams and disciplines contributing sensor, wake vortex modeling, and aircraft/wake vortex interaction modeling capabilities to the AVOSS. The motivation for this analysis is that the traditional method of characterizing wake vortex strength, circulation, presents severe limitations for practical use in an automated system. Circulation of a single vortex, as rigorously defined, cannot be measured by practical wake vortex sensors in the general case of a dual-vortex system. Since vorticity distribution of vortices may change as the wake decays, we must also define the scale length over which circulation or other strength measures must be estimated.

The results, although subject to verification through more rigorous and complete analysis,

indicates that a 5 to 10 meter average sensed circulation, as would be seen by an ideal sensor, provides a suitable wake vortex strength definition. This definition has a number of desirable characteristics:

1. This parameter can be estimated from remote sensor data without dependency on model fits or choice of model.
2. Estimation of this parameter does not require wake velocity measurements in the more difficult to measure core region or at large radii.
3. The strength measurement is less sensitive to the viewing angle of deployed sensors, compared to a larger radius estimate.
4. Researchers using analytical models to predict aircraft response can easily diagnose this strength parameter from their model conditions, or alternately fit their model parameters to produce any required strength.
5. The strength definition correlates well to the effects of wake encounters by a wide range of aircraft sizes, from turbo-prop commuters to heavy transports.

The data also suggests that some latitude in this definition is appropriate, due to low sensitivity of the results to small changes in the averaging interval. Sensed circulation values over ranges of 5 to 15 meters, for example, would also be a suitable strength definition. Care must be taken in the AVOSS system design and integration that all subsystems, wake predictors, wake sensors, and aircraft/wake encounter analysis, use the same definition of strength.

References

1. Hinton, David A.: *Aircraft Vortex Spacing System (AVOSS) Conceptual Design*, NASA TM-110184, August 1995.

2. Hinton, D.A.: *An Aircraft Vortex Spacing System (AVOSS) For Dynamical Wake Vortex Spacing Criteria*, AGARD 78th Fluid Dynamics Panel Meeting and Symposium on the Characterisation & Modification of Wakes from Lifting Vehicles in Fluids, Trondheim, Norway, 20-23 May, 1996, AGARD CP-584, Paper 23.

3. Lamb, H.: *Hydrodynamics*, 6th Ed., Cambridge University Press, 1932.

4. Burnham, D.C. and Hallock, J.N.: *Chicago Monostatic Acoustic Vortex Sensing System, Volume IV: Wake Vortex Decay*, DOT/FAA/RD-79-103 IV, July 1982.

5. Hoffmann, E.R. and Joubert, P.N.: Turbulent Line Vortices, *J. of Fluid Mechanics* 16:395-411, 1963.

6. Garodz, Leo J. and Clawson, Kirk: *Vortex Wake Characteristics of B757-200 and B767-200 Aircraft using the Tower Fly-By Technique, Volume 1 and 2*, NOAA TM-ERL-ARL-199, January 1993.

7. Proctor, F.H.: *Numerical Simulation of Wake Vortices Measured During the Idaho Falls and Memphis Field Programs.* AIAA 96-2496, 14th AIAA Applied Aerodynamics Conference Proceedings Part-2, June 17-20, 1996, pgs. 943-960; New Orleans, LA.

8. Switzer, George F.: *Validation Tests of TASS for Application to 3-D Vortex Simulations*, NASA CR-4756, October 1996.

9. Proctor, F.H.; Hinton, D.A.; Han, J.; Schowalter, D.G.; and Lin, Y.-L.: *Two Dimensional Wake Vortex Simulations in the Atmosphere: Preliminary Sensitivity Studies*, AIAA 97-0056, Presented at the 35th Aerospace Sciences Meeting & Exhibit, January 9-10, 1997, Reno, NV.

10. Delisi, Donald P.; Robins, Robert E.; and Altman, Donald B.: *Laboratory and Numerical Studies of Vortex Evolution in Ideal and Realistic Environments*, Proceedings of the Aircraft Wake Vortices Conference, Vol. 2, Washington, D.C., October 29-31, 1991, DOT/FAA/SD/92-1.11, June 1992.

11. Hallock, J.N. and Burnham, D.C.: *Decay Characteristics of Wake Vortex from Jet Transport Aircraft*, AIAA 97-0060, 35th Aerospace Sciences Meeting & Exhibit, January 9-10, 1997, Reno, NV.

12. Greene, George C.: An Approximate Model of Vortex Decay in the Atmosphere, *Journal of Aircraft*, Vol. 23, No. 7, July 1986, pp. 566-573.

13. Liu, HT; Hwang, PA; and Srnsky, RA: Physical Modeling of Ground Effects on Vortex Wakes, *Journal of Aircraft*, Vol. 29, No. 6, Nov - Dec 1992.

14. Corjon, A.; Zheng, Z. C.; and Greene, G. C.: *Model of the Behavior of Aircraft Wake Vortices Experiencing Crosswind Near the Ground.* AIAA 96-2516, 27th AIAA Fluid Dynamics Conference, June 17-20, 1996; New Orleans, LA.

15. Zak, Allen J. and Rodgers, William G. Jr.: *Documentation of Atmospheric Conditions During Observed Rising Aircraft Wakes*, NASA Contractor Report 4767, April 1997.

16. Campbell, S.; Dasey, T.; Freehart, R.; Heinrichs, R.; Matthews, M.; and Perras, G.: *Wake Vortex Field Measurement Program at Memphis, TN.*, AIAA 96-0399, Presented at the 34th Aerospace Sciences Meeting & Exhibit, Reno, NV, 15-18 January, 1996.

17. Campbell, S.D.; Dasey, T.J.; Freehart, R.E.; Heinrichs, R.M.; Matthews, M.P.; Perras, G.H.; Rowe, G.S.: *Wake Vortex Field Measurement Program at Memphis, TN Data Guide*, Lincoln Laboratory Project Report NASA/L-2, January 14, 1997. Also published as NASA CR-201690, April 1997.

18. Perry, R. Brad; Hinton, David A.; and Stuever, Robert A.: *NASA Wake Vortex Research for Aircraft Spacing*, AIAA 97-0057, 35th Aerospace Sciences Meeting & Exhibit, January 9-10, 1997, Reno, NV.

19. Vicroy, D.; Brandon, J.; Greene, G.; Rivers, R.; Shah, G.; Stewart, E.; and Stuever, R.: *Characterizing the Hazard of a Wake Vortex Encounter*, AIAA 97-0055, 35th Aerospace Sciences Meeting & Exhibit, January 9-10, 1997, Reno, NV.

20. Sammonds, Robert I.; Stinnett, Glen W. Jr.; and Larson, William E.: Criteria Relating Wake Vortex Encounter Hazard to Aircraft Response, *Journal of Aircraft*, Vol. 14, No. 10, October 1977.

21. Tatnall, C.R., *A Proposed Methodology for Determining Wake-Vortex Imposed Aircraft Separation Constraints*, Master of Science Thesis, The School of Engineering and Applied Science of The George Washington University; Directed by Dr. Roland Bowles, August 1995.

22. Condit, P.M. and Tracy, P.W.: *Results of the Boeing Company Wake Turbulence Test Program, , Published in Aircraft Wake Turbulence and its Detection*, Proceedings of a Symposium on Aircraft Wake Turbulence, Seattle, Washington, September 1-3, 1970.

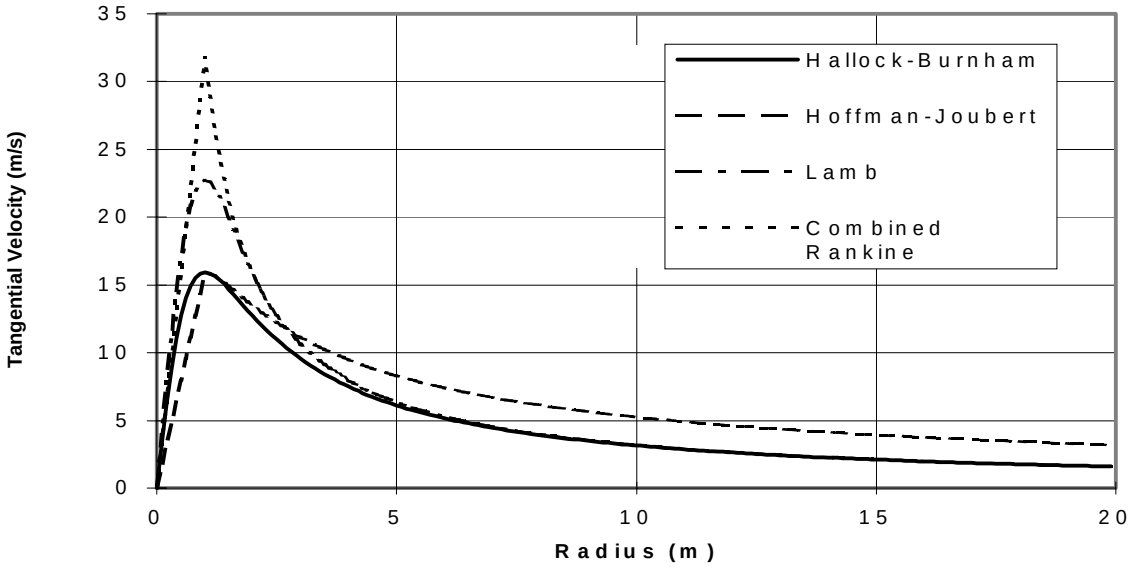

Figure 1 - Velocity Profiles for Four Wake Models

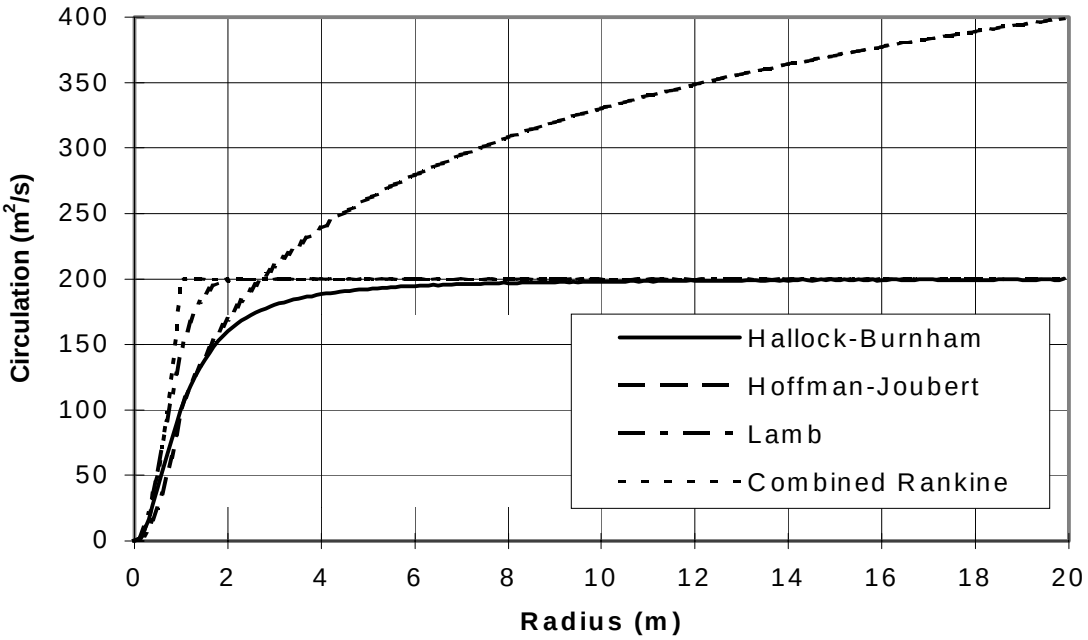

Figure 2 - Circulation Profiles for Four Wake Models

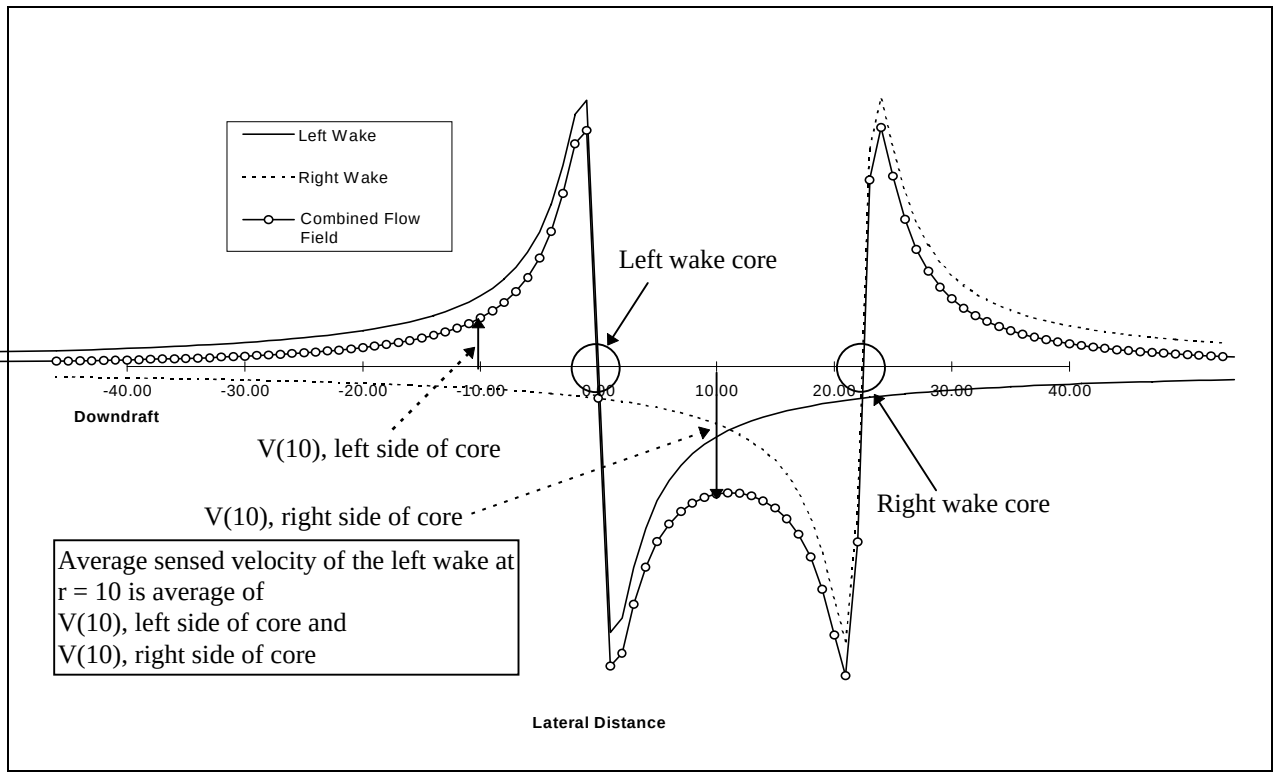

Figure 3 - Relationship of Individual Wake Vertical Velocities and Observed Vertical Velocity, as Viewed from Below.

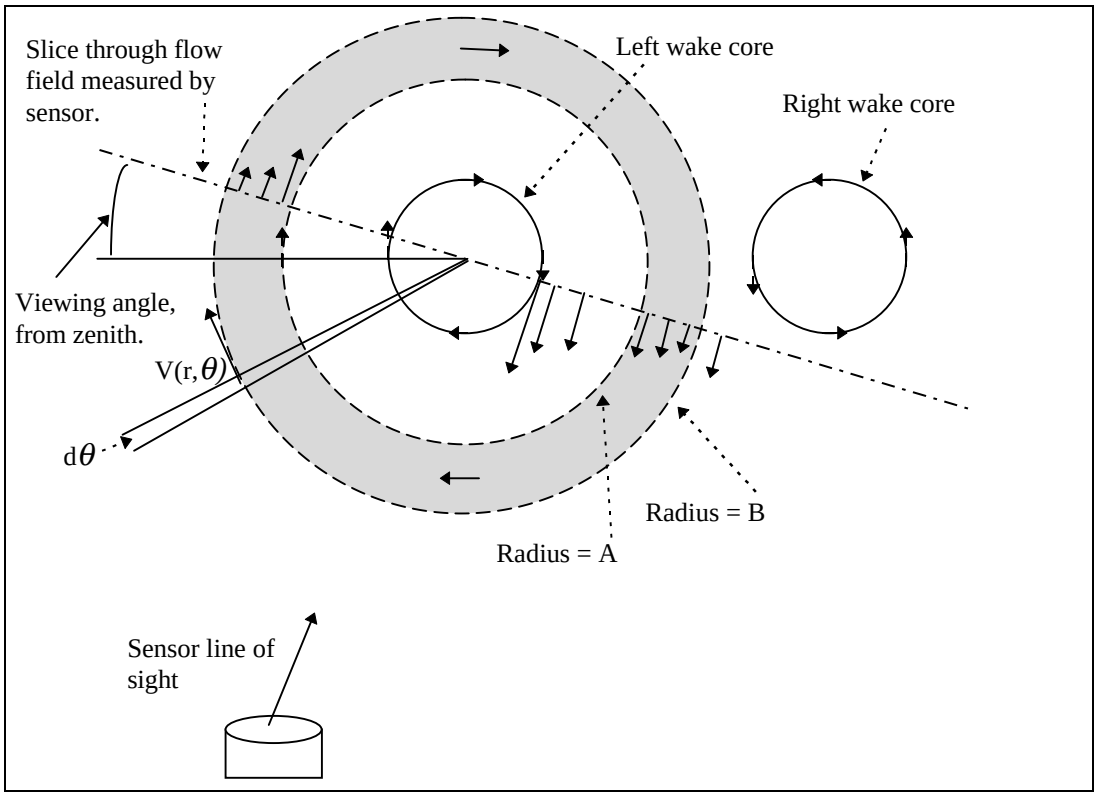

Figure 4 - Geometry Relating Circulation and Sensed Circulation

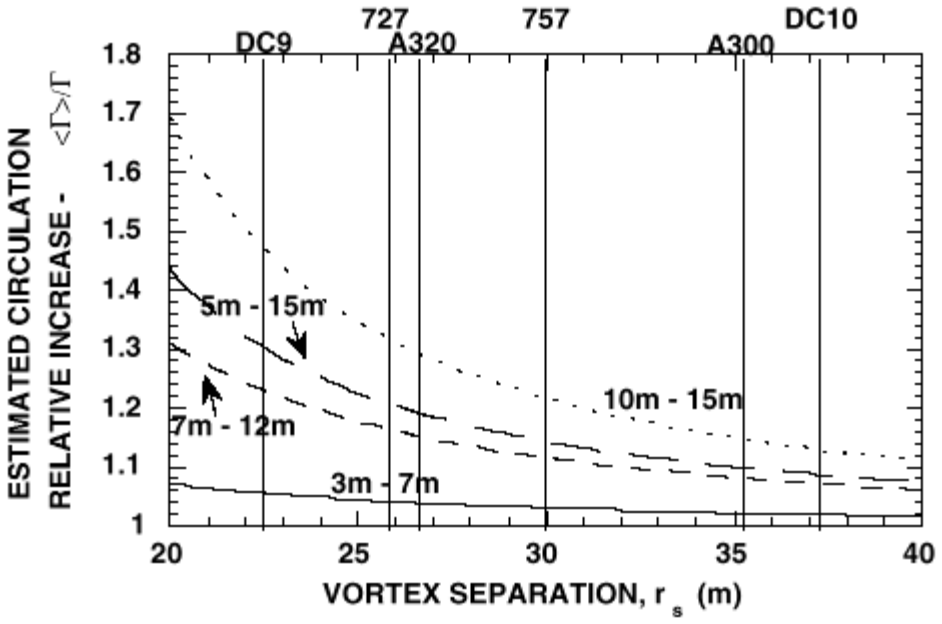

Figure 5 - Relationship between Observed and Single Vortex Circulation with Variations in Circulation Averaging Interval and Wake Spacing (reproduced from reference 17).

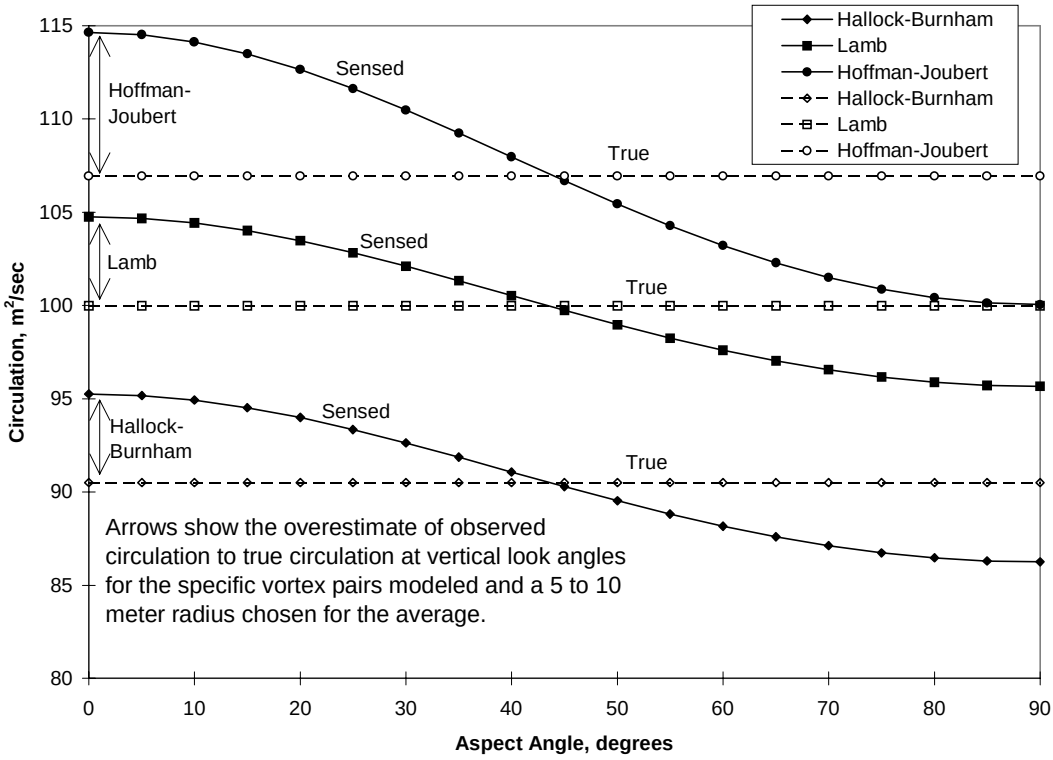

Figure 6 - Relationship Between True and Observed Circulation with Change in Viewing Angle.

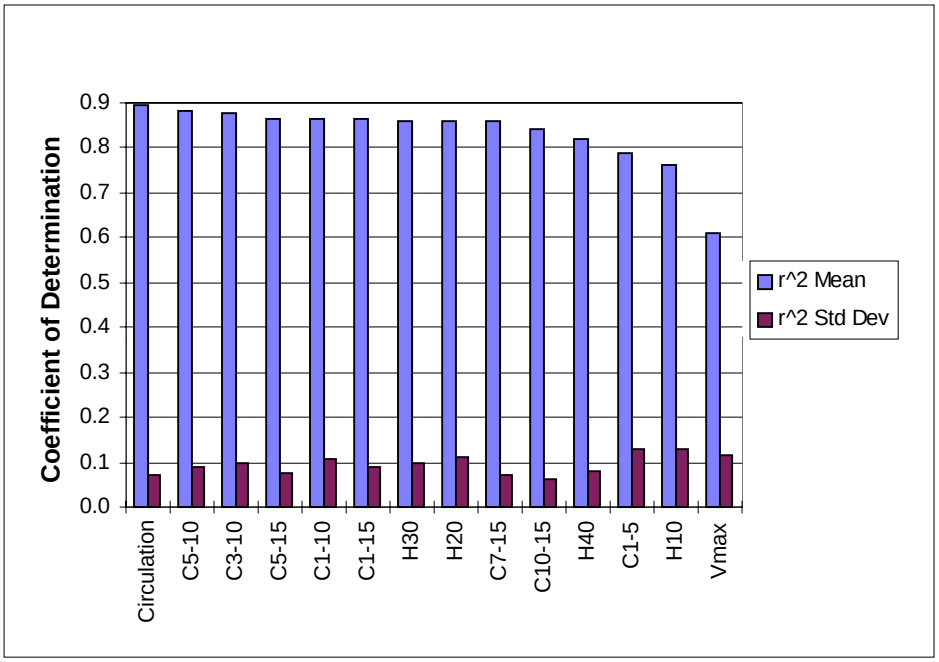

Figure 7 - Mean and Standard Deviation of Coefficient of Determination for all Wake Encounter Cases.

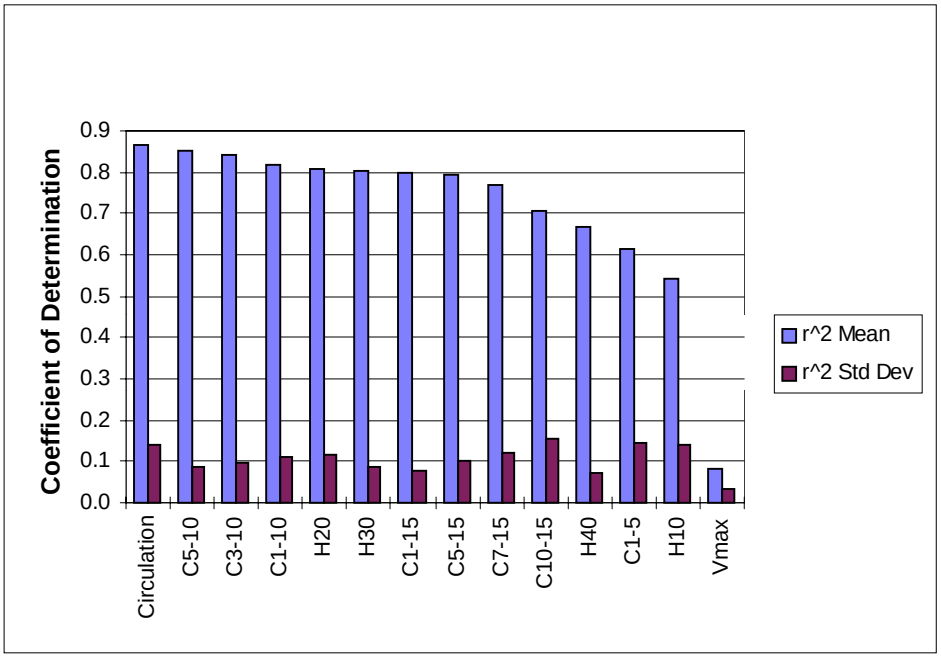

Figure 8 - Mean and Standard Deviation of Coefficient of Determination for all Full-Strength Wake Encounter Cases.

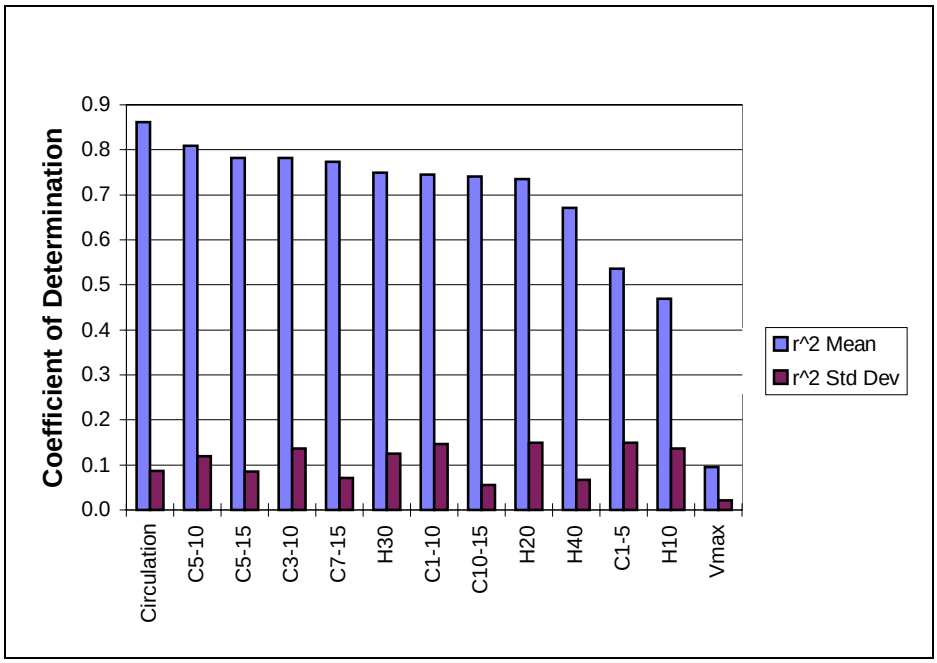

Figure 9 - Mean and Standard Deviation of Coefficient of Determination for all One-Half Strength Wake Encounter Cases.

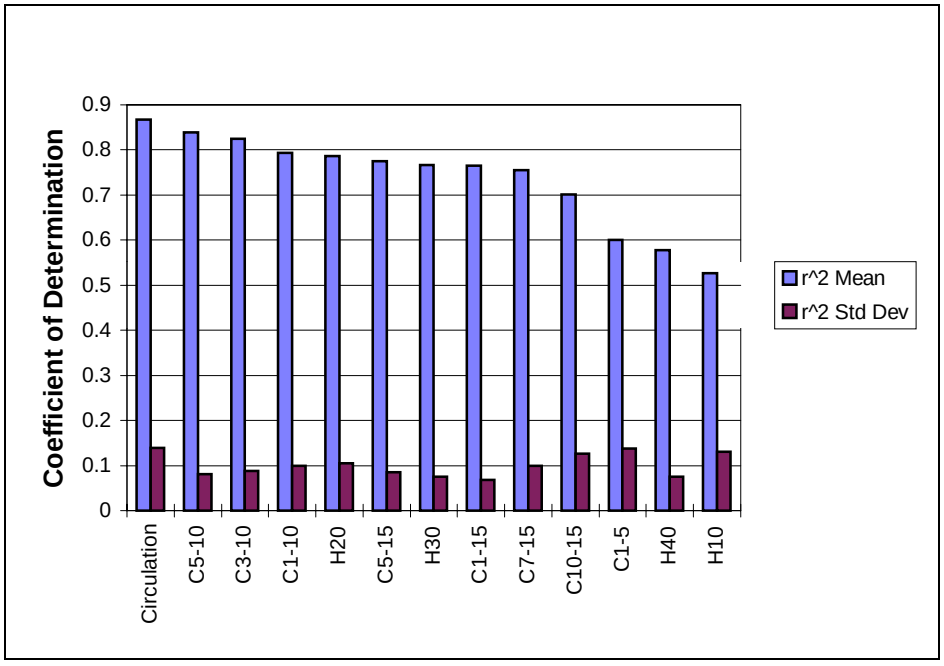

Figure 10 - Mean and Standard Deviation of Coefficient of Determination for Vertical Viewing Angle Wake Encounter Cases.

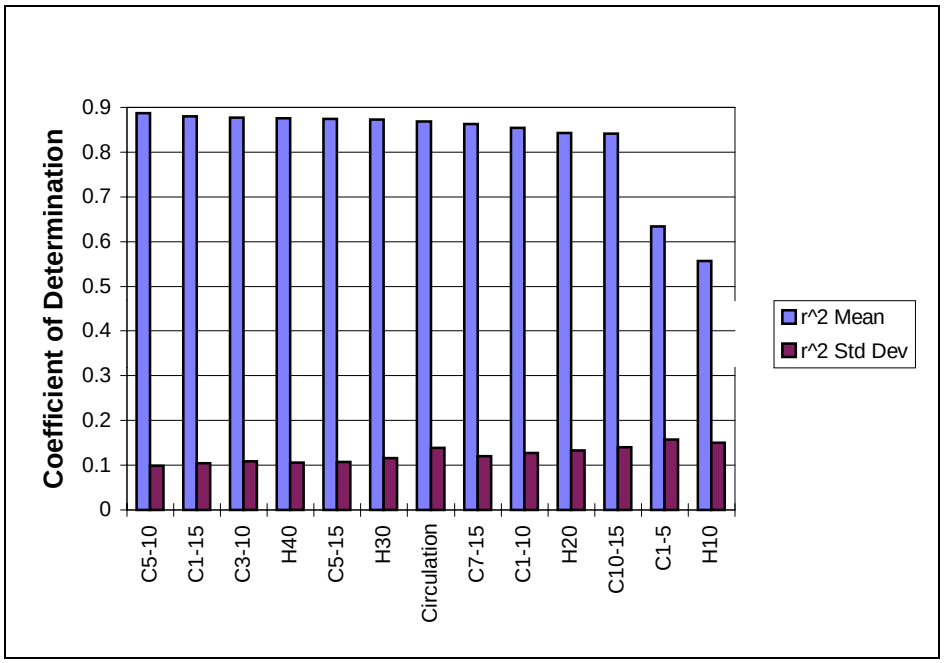

Figure 11 - Mean and Standard Deviation of Coefficient of Determination for 80^{o} Viewing Angle (10^{o} above Horizon) Wake Encounter Cases.

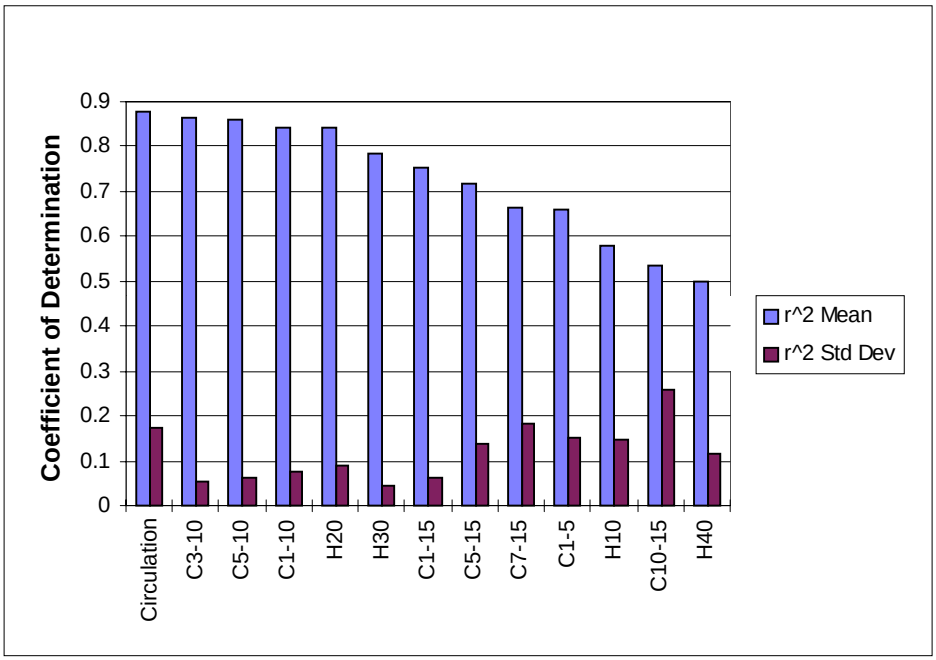

Figure 12 - Mean and Standard Deviation of Coefficient of Determination for Default Core Spacing Wake Encounter Cases.

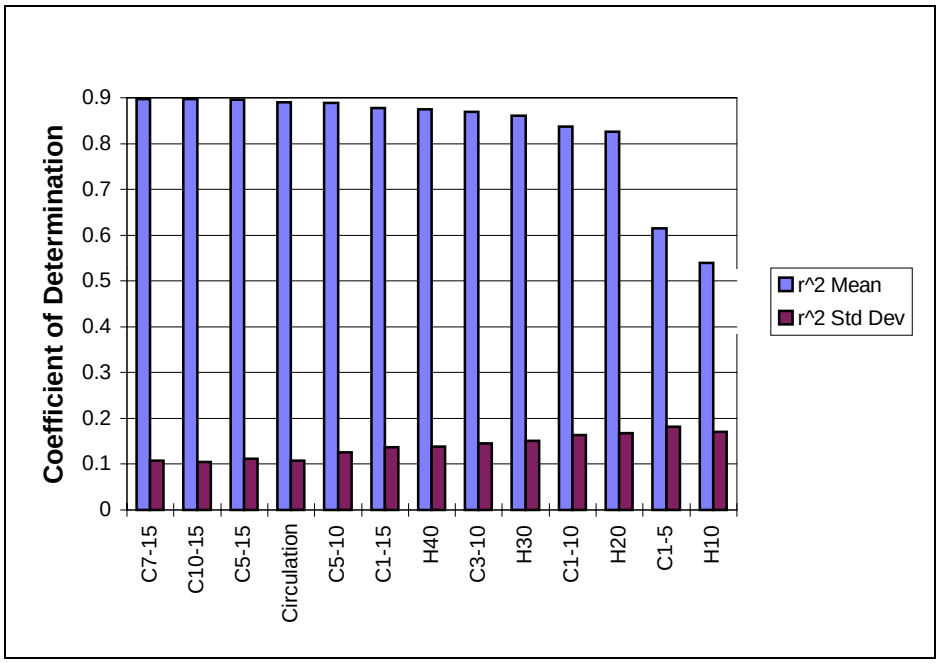

Figure 13 - Mean and Standard Deviation of Coefficient of Determination for Very Large Core Spacing Wake Encounter Cases.

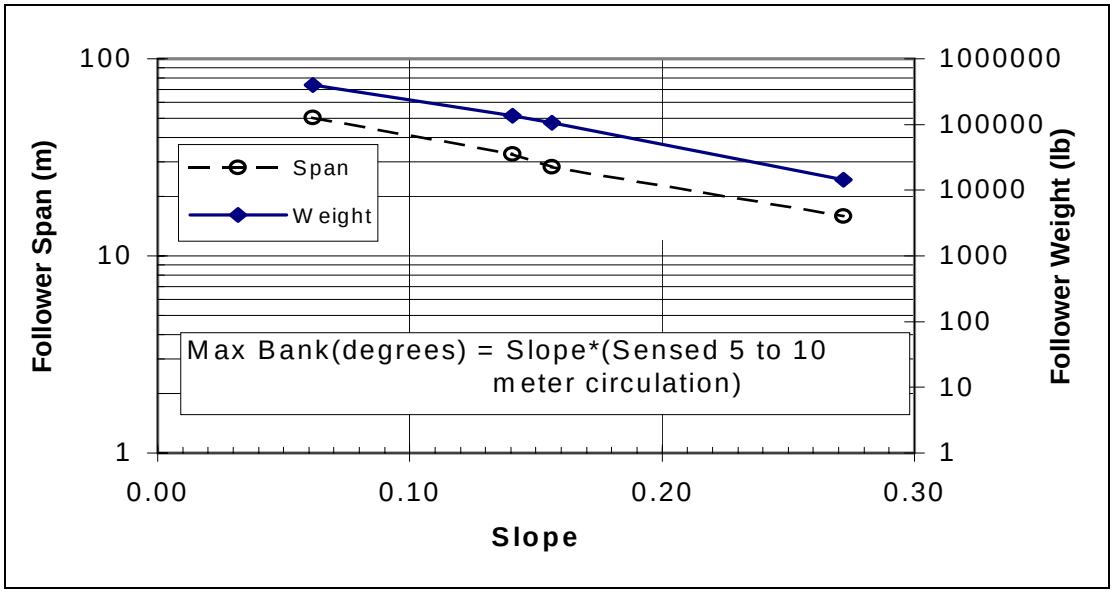

Figure 14 - Relationship of Maximum Bank Angle to 5-10 Meter Average Sensed Circulation and Encounter Airplane Weight and Span.

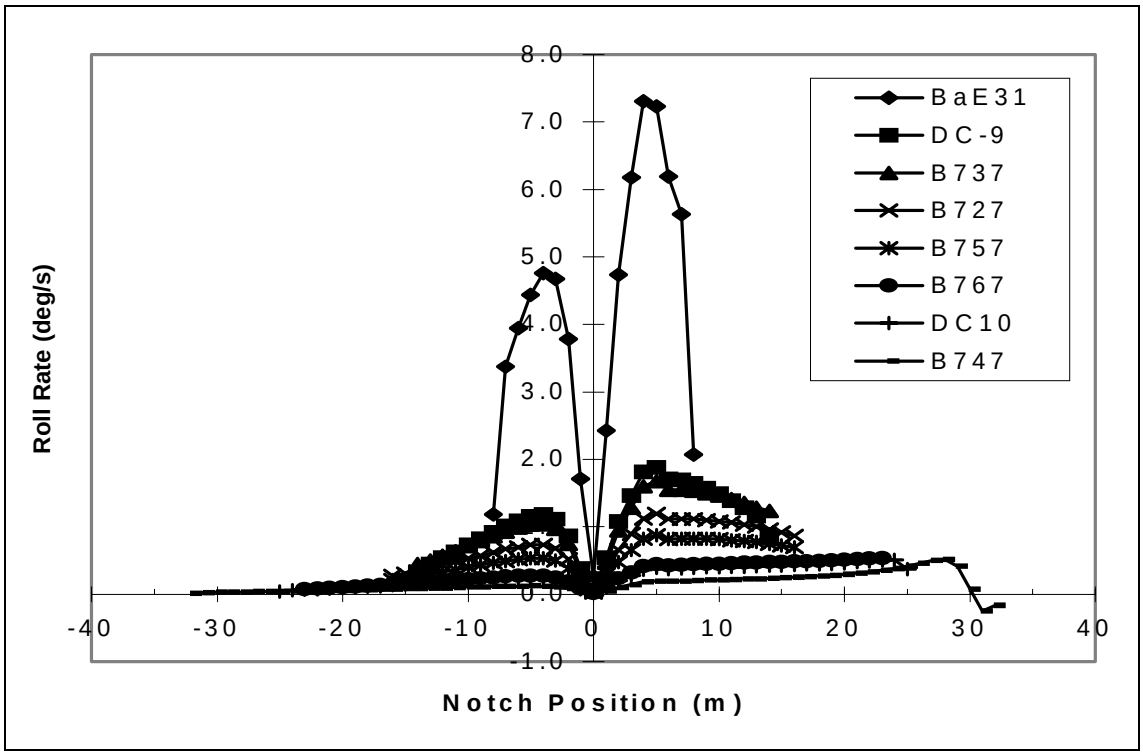

Figure 15 - Quasi-Steady Roll Rate Variation with Position of Wake Vortex Notch Filter for Eight Follower Aircraft.

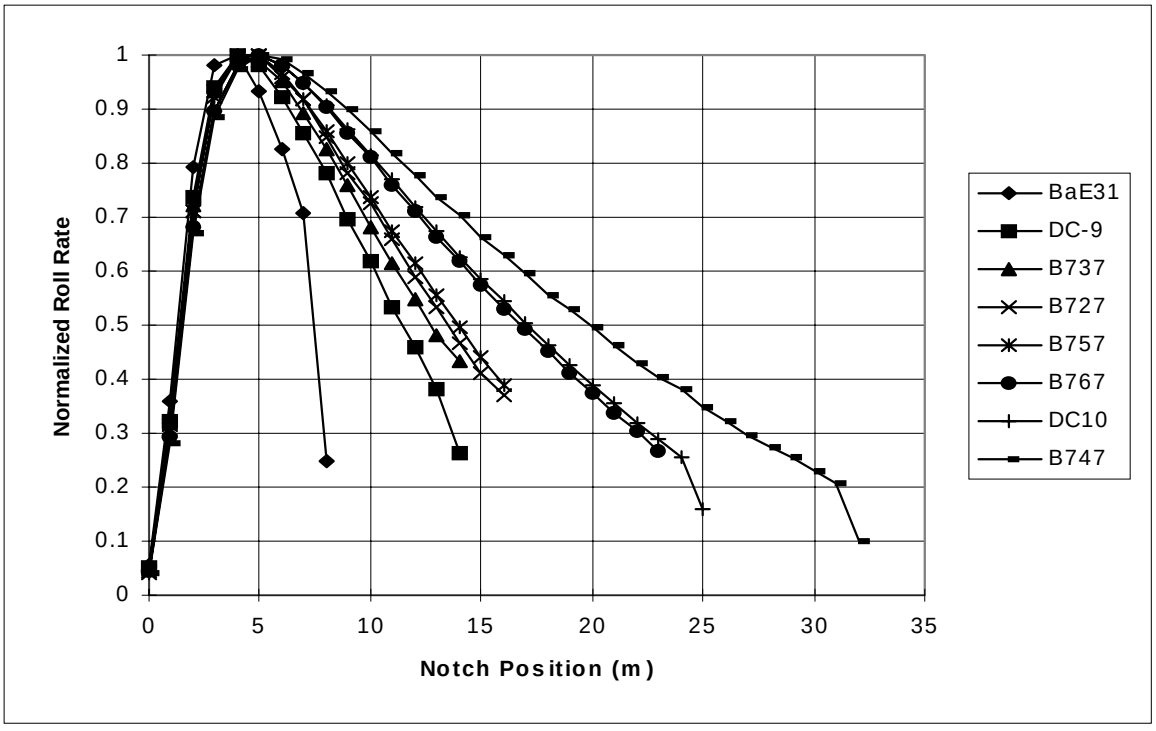

Figure 16 - Normalized Quasi-Steady Roll Rate Variation with Radius of Wake Vortex Notch Filter for Eight Follower Aircraft.

Appendix A - Wake Vortex Model Equations

The following four wake vortex models are frequently used to model wake velocity fields for analytical aircraft upset predictions, for model fits to interpret field measurements, or for potential flow models used to predict wake vortex motion. Initialization of a model to represent a wake from a given aircraft is generally performed by assuming a core radius, normally as some percentage of the generating wing span, and setting model circulation equal to the theoretical aircraft wake circulation. This model circulation, for all wakes except the Hoffman-Jourbert, is found by taking the limit of circulation as radius approaches infinity.

Hallock-Burnham:

$$V(r) = \frac{\Gamma_\infty}{2\pi}\frac{r}{r^2 + r_c^2}$$

$$\Gamma(r) = \frac{\Gamma_\infty r^2}{r^2 + r_c^2}$$

Lamb:

$$V(r) = \frac{\Gamma_\infty\left(1 - e^{-1.2526\left(\frac{r}{r_c}\right)^2}\right)}{2\pi r}$$

$$\Gamma(r) = \Gamma_\infty\left(1 - e^{-1.2526\left(\frac{r}{r_c}\right)^2}\right)$$

Combined-Rankine:

The Combined-Rankine model is simply a solid body rotation inside the core radius, and a 1/r velocity profile beyond the core radius.

$$V(r) = V_c\left(\frac{r}{r_c}\right)$$

$$\Gamma(r) = \Gamma_c\left(\frac{r}{r_c}\right)^2 \qquad \text{For } r \le r_c$$

$$V(r) = V_c\left(\frac{r_c}{r}\right)$$

$$\Gamma(r) = \Gamma_c \qquad \text{For } r > r_c$$

or in terms of the circulation at infinity:

$$V(r) = \frac{\Gamma_\infty}{2\pi}\left(\frac{r}{r_c^2}\right)$$

$$\Gamma(r) = \Gamma_\infty\left(\frac{r}{r_c}\right)^2 \qquad \text{For } r \le r_c$$

$$V(r) = \frac{\Gamma_\infty}{2\pi r}$$

$$\Gamma(r) = \Gamma_\infty \qquad \text{For } r > r_c$$

Hoffman-Joubert:

Since the circulation is not bounded as the radius approaches infinity, the velocity profile of the Hoffman-Joubert model is presented in terms of the core velocity and core circulation.

$$V(r) = V_c\left(\frac{r}{r_c}\right)$$

$$\Gamma(r) = \Gamma_c\left(\frac{r}{r_c}\right)^2 \qquad \text{For } r \le r_c$$

$$V(r) = V_c\left[\frac{1 + \ln\left(r/r_c\right)}{r/r_c}\right]$$

$$\Gamma(r) = \Gamma_c\left[1 + \ln\left(r/r_c\right)\right] \qquad \text{For } r > r_c$$

Appendix B - Derivation of the Strength Factor H(B)

One approach to quantifying the strength of a vortex pair is to abandon the circulation estimation attempts and compute a parameter that would directly relate to the rolling moment of a wing immersed in the flow. This is not to be confused with an "acceptable encounter definition". The acceptability of an encounter will depend not only on instantaneous rolling moment but also on the aircraft moments of inertia, roll control authority, assumed pilot response delays, and aircraft altitude at the encounter. The proposed index is strictly a strength parameter for the vortex itself.

The rolling moment on a wing immersed in a rotating flow field may be computed by integrating the product of the flow-field induced lift change at each distance from the wind center and the distance to that station. Reference 22 provides the basic equations for this calculation. The equations are presented here with modifications for non-symmetric flow about the aircraft longitudinal axis and to remove aircraft roll rate effects on rolling moment:

$$R = \int_{-b/2}^{b/2} L r dr \qquad \text{(B1)}$$

where R is the rolling moment, b is aircraft wing span, and L is the section lift change induced by the wake vortex. The section lift change is:

$$L = c_{L_\alpha} \Delta\alpha q c(r) \qquad \text{(B2)}$$

where $C_{L\alpha}$ is the wing lift curve slope, assumed to be constant across the wing span, $\Delta\alpha$ is the change in angle of attack induced by the wake vortex, q is the dynamic pressure, and c(r) is the wing chord at any radius. The change in local angle of attack due to the wake vortex, using small angle approximation, is:

$$\Delta\alpha = \frac{V(r)}{V_a} \qquad \text{(B3)}$$

where V(r) is the wake vortex velocity component normal to the wing plane at distance r from the wing center station and V_a is the aircraft airspeed. Substituting (B2) and (B3) into (B1) gives:

$$R = \frac{C_{L_\alpha} q c_{root}}{V_a} \int_{-b/2}^{b/2} \left[1 - \frac{2|r|(1-\lambda)}{B}\right] V(r) r dr \qquad \text{(B4)}$$

where c(r) has been replaced with the root chord c_{root} and the percent of wing chord expressed by the taper ratio λ. At r = 0 this percent is 1, and at r = B/2 the percent of chord is λ.

This equation is a function both of the wake vortex velocity profile normal to a tapered plate of span B, and the aircraft specific properties of that plate including C_{La}, airspeed, and root chord. The proposed strength index makes use of the vortex specific terms while essentially neglecting the aircraft specific terms. The proposed wake vortex strength index is:

$$H(B) = \int_{-B/2}^{B/2} \left[1 - \frac{2|s|(1-\lambda)}{B}\right] V(s) s ds \qquad \text{(B5)}$$

The strength index is essentially the second moment of the flow field about the reference plate and can be directly related to rolling moment. One term remains that is potentially aircraft specific, the plate taper ratio. Examination of aircraft data indicates that most aircraft of given span ranges tend to have very similar taper ratios. Table B1 summarizes the span and taper ratio for 67 aircraft, as compiled from numerous data sources by Robert Stuever of NASA Langley. Since larger taper ratios are more conservative the value chosen for each grouping was biased strongly towards the larger values within the group. When lumped into span categories of 10, 20, 30, and 40 and above meters, chosen values for the taper ratio came to 1.0, 1.0, 0.5, and 0.3 respectively. Computing the strength index over a 10 meter span would represent the hazard to a small general aviation aircraft while 30 and 40 meter spans represent most commercial transports in the large category, that would be most susceptible to wake upsets. Computing a strength index at span lengths greater than 40 meters may not be practical due to low vortex velocity to ambient wind ratios at the larger radii and other limitations in sensor measurement capability.

Table B1 - Taper Ratio Groupings for 67 Aircraft - part 1 of 2.

Span Group	Wing Span (meters)	Taper Ratio	Aircraft Type	Group Taper Range	Group Ratio Average
	10.0	1	Piper Cherokee Lance		
	10.2	0.5	Beech Bonanza 36		
	10.9	0.7	Cessna 172		
	11.3	0.67	Cessna 310		
	11.5	0.42	Beech Baron 58		
10 meter	12.0	0.56	Learjet 35a	0.31 to 1.0	0.53, n=11
	13.3	0.35	Beech Jet 400A		
	13.3	0.43	Learjet 31A		
	14.0	0.5	Beech King Air B100		
	14.3	0.41	Learjet 60		
	14.5	0.31	Piper Cheyenne 400		
	15.9	0.38	BAe Super31		
	15.9	0.62	Cessna 208A Caravan I		
	15.9	0.31	Cessna 550 Citation II		
	15.9	0.3	Cessna 560 Citation V		
	16.6	0.42	Beech 1900C		
	17.0	0.71	Dornier 228-100		
	17.4	0.33	Fairchild SA-227 Metro		
	17.7	0.41	Beech Super King Air 350		
	18.9	0.29	Dassault-Breguet Falcon 50		
	19.5	0.28	Cessna 750 Citation X		
20 meter	19.6	0.32	Challenger 601-3A	0.25 to 1.0	0.47, n=21
	19.8	0.5	EMB-120 Brasilia		
	19.8	1	DHC-6 Twin Otter		
	21.0	0.73	Dornier 328		
	21.2	0.25	Canadair Regional Jet		
	21.4	0.42	Saab 340B		
	22.1	0.49	Antonov An-38		
	22.8	0.83	Shorts 330-200		
	23.5	0.31	Gulfstream IV		
	24.6	0.55	ATR-42-300		
	24.8	0.38	Saab 2000		

Table B1 - Taper Ratio Groupings for 67 Aircraft - Concluded

Span Group	Wing Span (meters)	Taper Ratio	Aircraft Type	Group Taper Range	Group Ratio Average
	25.1	0.32	Fokker F-28-4000		
	25.8	0.4	Airtech Cn-235		
	27.1	0.55	ATR-72		
	27.4	0.48	DHC-8 Dash 8		
	28.1	0.2	Fokker F-100		
	28.4	0.34	Boeing 737-200		
	28.5	0.24	McD DC-9-50		
30 meter	29.0	0.4	Fokker F-50	0.16 to 0.55	0.32, n=16
	29.2	0.33	Antonov An-32		
	31.9	0.3	Antonov An-74		
	32.9	0.16	McD MD-81		
	32.9	0.3	Boeing 727-100 Basic		
	32.9	0.3	Boeing 727-200		
	33.9	0.25	Airbus A320-100		
	34.1	0.24	Airbus A321		
	34.9	0.3	Yakovlev Yak-42		
	37.6	0.21	Tupolev Tu-154M		
	38.0	0.23	Boeing 757-200		
40 meter	42.0	0.23	Tupelov Tu-204	0.21 to 0.28	0.25, n=6
	43.9	0.26	Airbus A310-200		
	44.5	0.28	Boeing 707		
	44.8	0.27	Airbus A300-600		
	47.3	0.3	McD DC-10-10		
	47.4	0.3	Lockheed L1011-500		
	47.6	0.27	Boeing 767-200ER/-300		
50 meter	48.1	0.27	Ilyushin II-86	0.25 to 0.32	0.28, n=8
	50.1	0.3	Lockheed L1011-500EW		
	50.4	0.25	McD DC-10-30		
	50.5	0.32	Ilyushin II-76T		
	51.7	0.26	McD MD-11		
	57.7	0.26	Ilyushin II-96		
	59.6	0.23	Airbus A330		
60 meter	59.7	0.25	Boeing 747-100	0.20 to 0.26	0.24, n=5
	61.0	0.2	Boeing 777-200		
	64.3	0.25	Boeing 747-400		

Appendix C- Overview of Aircraft Model Used in Bank Angle Response Calculations

The computation of maximum roll response for a given encounter was accomplished by applying static models for induced lift and roll moment to a 3-DOF dynamic model which allows the following aircraft to bank and translate both vertically and laterally (forward speed is assumed constant). The wake itself is modeled as a pair of stationary 2-D Burnham-Hallock vortices located at +/- s along the inertial Y-axis, with core radii of r_c = 5% of the generating aircraft's wing span. Although the standard value of vortex-pair separation for elliptically loaded wings was used (s = $b_g(\pi/8)$), a value of s = $b_g(300)$ was used to simulate an isolated vortex. This value has no particular significance; it was found to be adequate through trial-and-error. For purposes of modeling the induced lift and roll moment, the following aircraft is simplified to a flat, linearly-tapered wing which extends to the aircraft centerline (i.e. fuselage is neglected). However, the dynamic model is run with whole-aircraft characteristics such as weight, I_{XX}, roll damping, and roll control. In these calculations, 75% of the max. landing weight (and corresponding I_{XX} values) are used for both the following and leading aircraft. In determining the wake characteristics, the leading aircraft is assumed to have an elliptical lift distribution.

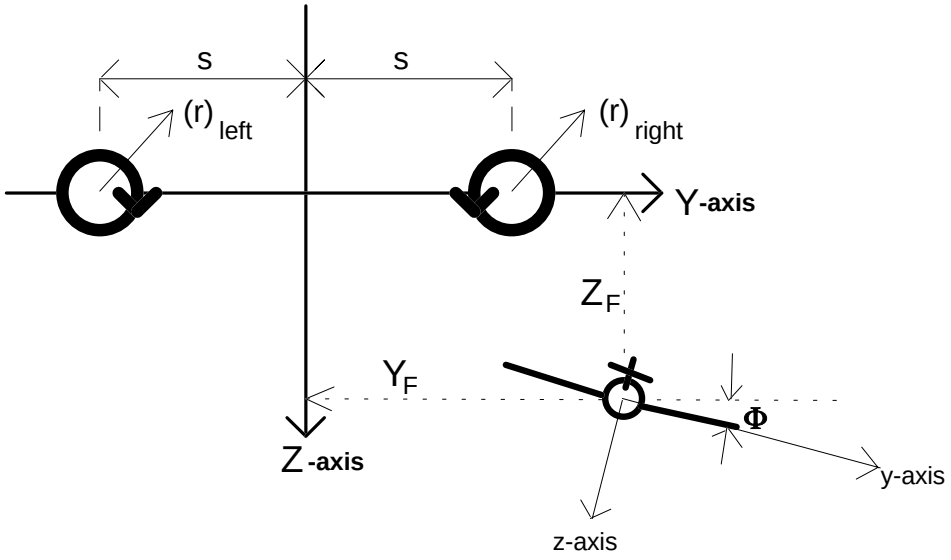

Summary of Induced Load Models

The induced lift and roll moment were found with a quasi-strip-theory method in which the strips are infinitesimal, so that analytical expressions can be obtained. In coefficient form, the induced lift and roll moment are, respectively:

$$C_{L_V} = K_{L_V}\left(I_1 - I_2\right) \text{ , where}$$

$$K_{L_V} = -\left(\frac{2}{\pi^2}\right)\left(\frac{C_{L_G} C_{L_{\alpha F}}}{(AR)_G}\right)\left(\frac{b_G}{b_F}\right)\left(\frac{1}{1+\lambda_F}\right)\left(\frac{V_{a_G}}{V_{a_F}}\right)$$

$$I_i = \frac{1}{2}\left(C_i\Omega - 1\right)\ln\left[\frac{{C_i}^2 + {A_i}^2}{\left(C_i - D\right)^2 + {A_i}^2}\right] + \frac{1}{2}\left(C_i\Omega + 1\right)\ln\left[\frac{{C_i}^2 + {A_i}^2}{\left(C_i + D\right)^2 + {A_i}^2}\right]$$
$$+ A_i\Omega\left[2\tan^{-1}\left(\frac{C_i}{A_i}\right) - \tan^{-1}\left(\frac{C_i - D}{A_i}\right) - \tan^{-1}\left(\frac{C_i + D}{A_i}\right)\right] \qquad i = 1,2$$

and the induced roll moment coefficient is

$$C_{\mathrm{L}_V} = K_{\mathrm{L}_V}\left(I_1 - I_2\right) \text{ , where}$$

$$K_{\mathrm{L}_V} = \left(\frac{2}{\pi^2}\right)\left(\frac{C_{L_G}C_{L_{\alpha F}}}{(AR)_G}\right)\left(\frac{b_G}{b_F}\right)^2\left(\frac{1}{1+\lambda_F}\right)\left(\frac{V_{a_G}}{V_{a_F}}\right)$$

$$I_i = \frac{1}{2}\left[\left({C_i}^2 - {A_i}^2\right)\Omega - C_i\right]\ln\left[\frac{{C_i}^2 + {A_i}^2}{\left(C_i - D\right)^2 + {A_i}^2}\right] + \frac{1}{2}\left[\left({C_i}^2\right.\right.$$
$$\left.\left. - {A_i}^2\right)\Omega + C_i\right]\ln\left[\frac{{C_i}^2 + {A_i}^2}{\left(C_i + D\right)^2 + {A_i}^2}\right] + A_i\left[4C_i\Omega\tan^{-1}\left(\frac{C_i}{A_i}\right)\right.$$
$$\left. + \left(1 - 2C_i\Omega\right)\tan^{-1}\left(\frac{C_i - D}{A_i}\right) - \left(1 + 2C_i\Omega\right)\tan^{-1}\left(\frac{C_i + D}{A_i}\right)\right] \qquad i = 1,2$$

For both cases, the following variables are defined:

$$C_1 = \left(\overline{Y}_F + \bar{s}\right)\cos(\Phi) + \overline{Z}_F\sin(\Phi) \ , \ C_2 = \left(\overline{Y}_F - \bar{s}\right)\cos(\Phi) + \overline{Z}_F\sin(\Phi)$$

$${A_1}^2 = \left[\left(\overline{Y}_F + \bar{s}\right)\sin(\Phi) - \overline{Z}_F\cos(\Phi)\right]^2 + \bar{r}_c^{\,2} \ , \ {A_2}^2 = \left[\left(\overline{Y}_F - \bar{s}\right)\sin(\Phi) - \overline{Z}_F\cos(\Phi)\right]^2 + \bar{r}_c^{\,2}$$

$$D = b_F \big/ 2b_G$$

$$\Omega = \frac{1 - \lambda_F}{D}$$

The overbar denotes normalization with the leading aircraft's wing span, and the subscripts F and G refer to the following and leading aircraft, respectively.

Summary of 3-DOF Dynamic Model

The governing equation set is

$$\dot{\bar{Y}}_{F_1} = \bar{Y}_{F_2}$$

$$\dot{\bar{Y}}_{F_2} = \left[\left(g + \left(\bar{q} S_F C_{L_V}\right)/m\right)\sin(\Phi)\right]/b_G$$

$$\dot{\bar{Z}}_{F_1} = \bar{Z}_{F_2}$$

$$\dot{\bar{Z}}_{F_2} = \left[g - \left(g + \left(\bar{q} S_F C_{L_V}\right)/m\right)\cos(\Phi)\right]/b_G$$

$$\dot{\Phi} = p$$

$$\dot{p} = \left(\frac{q S_F b_F}{I_{XX}}\right)\left[\left(\frac{p b_F}{2V_{aF}}\right)C_{l\hat{p}} + C_{lV} - C_{L_C}\,\mathrm{U}\left(t - T_C\right)\left(\Phi/|\Phi|\right)\right]$$

where m is the mass of the follower. Here the pilot model is incorporated in the last equation; after a given pilot response time T_C (0.6 seconds), full roll control is input in the direction which will bring wings level. The value of roll control is computed based on the empirical approximation that full roll control countered by the aircraft's roll damping will produce a steady-state roll rate of $\hat{p} = \left(p \cdot b_F\right)/\left(2 \cdot V_{aF}\right) = 0.07$. The initial conditions are

$$\begin{Bmatrix} \bar{Y}_{F_1} \\ \bar{Y}_{F_2} \\ \bar{Z}_{F_1} \\ \bar{Z}_{F_2} \\ \Phi \\ p \end{Bmatrix}_{t=0} = \begin{Bmatrix} \left[\bar{Y}_F @ \left(C_{L_V}\right)_{\max}\right] + \bar{r}_C \\ 0 \\ 0 \\ \left(V_{a_F} \cdot \tan 3^\circ\right)/b_G \\ 0 \\ 0 \end{Bmatrix}$$

and the system was integrated with a standard 4th-Order Runge-Kutta scheme and a stepsize of 0.03 seconds.